APPROXIMATE DESIGN ESTIMATES FOR PURE COMPONENT CONDENSERS

By

SURESH BALAKRISHNAN

Bachelor of Technology

Indian Institute of Technology

Bombay, India

1977

Submitted to the Faculty of the Graduate College
of the Oklahoma State University
in partial fulfillment of the requirements
for the Degree of
MASTER OF SCIENCE
July, 1979

APPROXIMATE DESIGN ESTIMATES FOR

PURE COMPONENT CONDENSERS

Thesis Approved:

Thesis Adviser

Dean of the Graduate College

PREFACE

The purpose of this study is to analyze the performance of pure component condensers and to present a rapid estimation procedure to design shell and tube heat exchangers for the condensation of pure components.

Various aspects involved in pure component condensation and two-phase flow are discussed. The effect of pressure drop on mean temperature differences and condensation heat transfer coefficient is discussed. Rapid estimation procedures for design of shell and tube condensers are presented. Finally, a discussion on optimization of condensers is presented.

I wish to express my sincere thanks to Dr. Kenneth J. Bell for his advice and guidance and to the School of Chemical Engineering for the financial support offered to me. I take this opportunity to thank Dr. Billy L. Crynes for his constant encouragement.

I wish to express my sincere gratitude to Dr. C. B. Panchal and Mr. Rajan N. Vaz for their help and encouragement. Finally, I wish to thank Mrs. Dolores Behrens for a typing job well done in such a short time.

TABLE OF CONTENTS

LIST OF TABLES

LIST OF FIGURES

NOMENCLATURE

A	- heat transfer area, ft^2
C	- clearance between adjacent tubes, in.
D	- diameter, in., D_i - inside diameter, D_o outside diameter, D_{otl} - diameter of outer tube limit, in.
d_o	- tube outside diameter, in.
F_1, F_2, F_3	- factors defined by Tables V, VI, VII, respectively
F_c	- fraction of total tubes that are in crossflow
F_{sbp}	- fraction of total crossflow area available for bypass flow around tube bundle
f	- friction factor, f_i - friction factor for ideal tube banks, f - shell side friction factor
G	- total mass velocity, $lb/ft^2hr.$
g	- gravitational acceleration, $ft./sec.^2$
g_c	- gravitational conversion constant, 4.17×10^8 $lbm.ft./lb_f$ hr^2

ΔH_v	- heat of vaporization, Btu/lb mole
h_c, h_i, h_o	- heat transfer coefficient for condensation, inside tubes, outside tubes; Btu/hrft^2^{o}F
K	- thermal conductivity, Btu/hrft^2^{o}F
L	- total length of tubes, ft.
LVF	- liquid volume fraction
ℓ	- effective tube length (between tube sheets), ft.
ℓ_c	- baffle cut, inc.
ℓ_s	- baffle spacing, in.
MTD	- mean temperature difference, ^{o}F
N_b	- number of baffles in the exchanger
N_c	- number of tube rows crossed during flow through one crossflow section
N_{cw}	- number of effective crossflow rows in each window
N_{ss}	- number of pairs of sealing strips or equivalent obstruction to bypass flow encountered by the stream in one crossflow section
N_t	- total number of tubes in the exchanger
P	- pressure, lb/in.^{2}
Pr_ℓ	- liquid phase Prandtl number

ΔP	- pressure drop, lb/in.^{2}
p	- tube pitch, in.
p_N	- tube pitch normal to flow, in.
p_p	- tube pitch parallel to flow, in.
Q	- total heat transfer rate, Btu/hr
R	- gas constant, 1.987 Btu/lb mole ^oR
R_b	- correction factor for effect of bundle bypass on pressure drop
Re	- Reynolds number
R_L	- correction factor for effect of baffle leakage on pressure drop
$R_{ST,CF}$	- correction factor for effect of bundle bypass and baffle leakage on pressure drop in two phase flow
$R_{ST,W}$	- correction factor for effect of baffle leakage on pressure drop in two phase flow
S_m	- crossflow area at or near centerline for one crossflow section, in.^{2}
S_{sb}	- shell-to-baffle leakage area for a single baffle, in.^{2}
S_{tb}	- tube-to-baffle leakage area for a single baffle, in.^{2}
S_w	- area for flow through window, in.^{2}

S_{wg} - window gross area, $in.^2$

S_{wt} - window area occupied by tubes, $in.^2$

T - temperature of shell-side fluid, ^oF, T_1 - inlet temperature, T_2 - outlet temperature, T_s - saturation temperature, T_w - wall temperature

t - temperature of tube=side fluid, ^oF t_1 - inlet temperature, t_2 - outlet temperature

U - overall heat transfer coefficient, $Btu/hrft^{2o}F$, U_o - based on tube outside area, U_i - based on tube inside area

V - velocity of fluid flow, ft/sec

W - weight flow rate lbs/hr

x - vapor quality (lb vapor/lb total)

Greek Letters

X_{tt}, $\Phi_{\ell tt}$ - Martinelli-Nelson factors

$\overline{\Phi^2_{\ell tt}}$ - multiplying factors in Figures 10, 11, 12, 13, 15

λ - latent heat of vaporization, Btu/lb

μ - viscosity, lb/fthr

ρ - density, lb/ft^3

Subscripts

c - condensing

CF - crossflow

f	- friction
g	- vapor phase
i	- inside
ℓ	- liquid phase
o	- outside
s	- shell-side
TPF	- two phase flow
t	- tube side
v	- vapor phase
w	- window

CHAPTER I

INTRODUCTION

The condensation of pure components occurs in a wide variety of applications in the process and related industries. Most common applications are the process condensers on distillation columns, on chemical reactors, power plant condensers and condensers used in refrigeration systems.

There are four basic mechanisms of condensation generally recognized: dropwise, filmwise, direct contact and homogeneous. Dropwise condensation, although alluring because of the high heat transfer coefficients reported in the literature, is not considered to be suitable for exploitation in the design of process condensers. Homogeneous condensation is primarily of concern in fog formation in equipment and is not a design mode by itself. Direct contact condensation, although a very efficient process, suffers from the disadvantage of mixing the condensate and the coolant. The most common mechanism of condensation found in process condensers is filmwise condensation. Therefore, all the attention in this thesis will be devoted to filmwise condensation, and all references to condensation will imply filmwise condensation, unless otherwise stated. The condensation of only pure components has been considered.

The subject of filmwise condensation may be further subdivided based on whether the vapor is condensing inside the tubes (in-tube)

or outside the tubes (in-shell) and whether the vapor hydrodynamics has any effect on the condensation process.

Regimes of Two-Phase Flow

The types and the detailed description of two-phase flows depends on the physical properties of the fluids flowing, the geometric configuration of the conduit and the kind of heat transfer process involved, if any. In the co-current flow of liquid and gas, there are four possible combinations of flow mechanisms: liquid turbulent/gas turbulent, liquid viscous/gas turbulent, liquid turbulent/gas viscous and liquid viscous/gas viscous (12). However, only two, namely liquid turbulent/gas turbulent and liquid viscous/gas turbulent have widespread applications in co-current contactors in the chemical industry. In addition, there may be several flow patterns depending upon the liquid and gas flow rates and also upon the type of the inlet.

Flow Patterns

The following general types of flow patterns are found in straight horizontal tubes (1):

1. Bubble flow-flow in which bubbles move along the upper part of the pipe at approximately the same velocity as the liquid.
2. Plug flow - flow in which alternate plugs of liquid and gas move along the upper part of the pipe.
3. Stratified flow - flow in which liquid flows along the bottom of the pipe and the gas flows above the liquid over a smooth interface.

4. Wavy flow - flow which is similar to stratified flow except that the gas flows at a higher velocity and the interface is disturbed by waves traveling in the direction of flow.
5. Slug flow - flow in which a wave of liquid is lifted up periodically by the more rapidly moving gas to form a frothy slug which moves more rapidly than the liquid.
6. Annular flow - flow in which the liquid flows in a film around the inside wall of the pipe and the gas flows at a higher velocity and in the central core of the pipe.
7. Spray or Mist flow - flow in which a large fraction of the liquid is entrained as a spray by the gas.

A modified form of the Baker map (2) is shown in Figure 1 and is useful in giving a general appreciation of the general kind of flow regime existing under given conditions. During the course of condensation, the relative ratios of vapor and liquid change; these changes may be conveniently followed on the Baker map with the aid of Figure 2, which is used in the following way: Calculate the values of the abscissa and ordinate on the Baker map corresponding to the half condensed point. Plot this point on Figure 1. Place the 0.5 point of the curve of Figure 2 on top of the point plotted on Figure 1 so that the coordinates are parallel on the two figures. Then the curve on Figure 2 traces the sequence of flow regimes as a function of vapor quality from pure vapor at the left infinity point to pure liquid at the bottom infinity.

For two-phase flow inside vertical tubes, the stratified and wavy flow regimes cannot exist and the flow regimes generally recognized in this case are bubble (low vapor rate), slug, annular, and

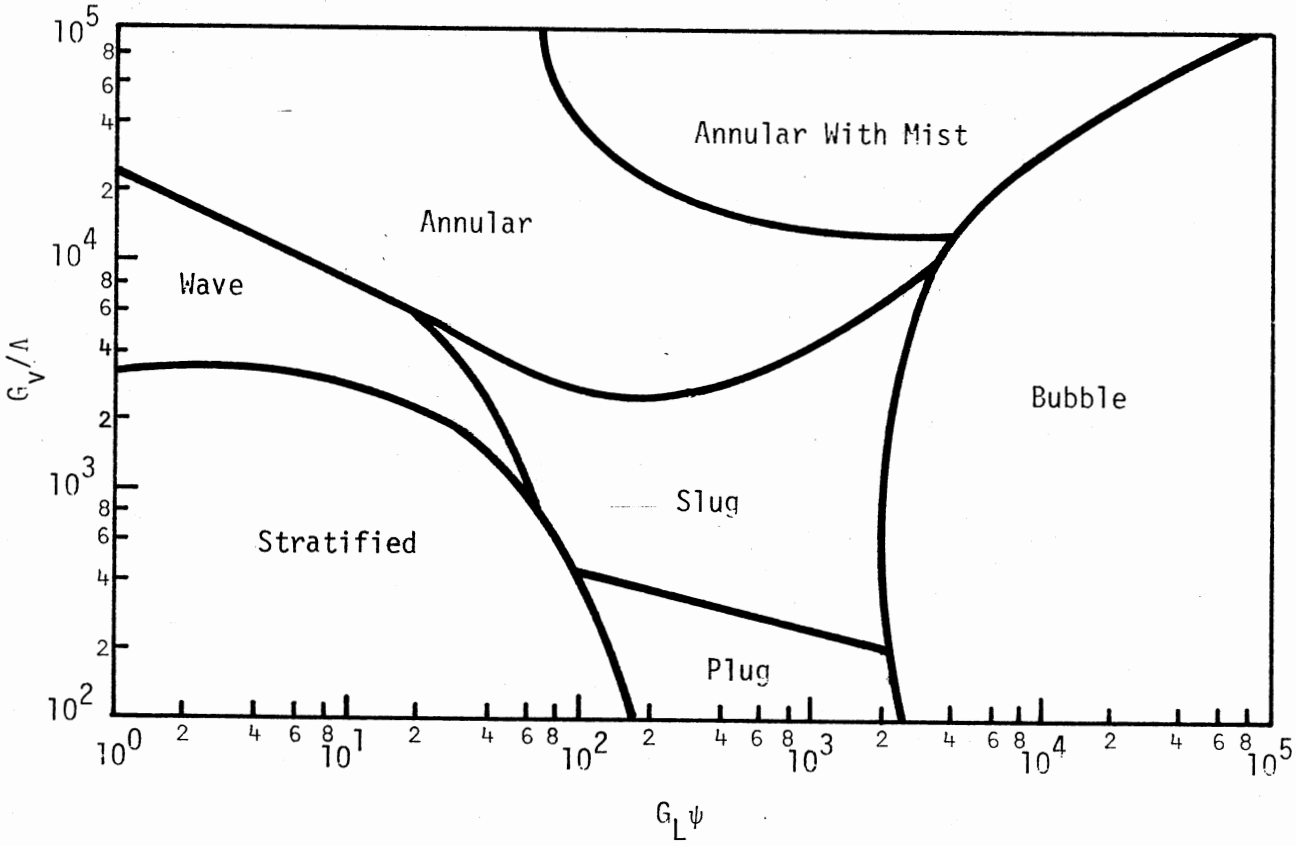

Figure 1. Transformed Baker Flow Regime Map

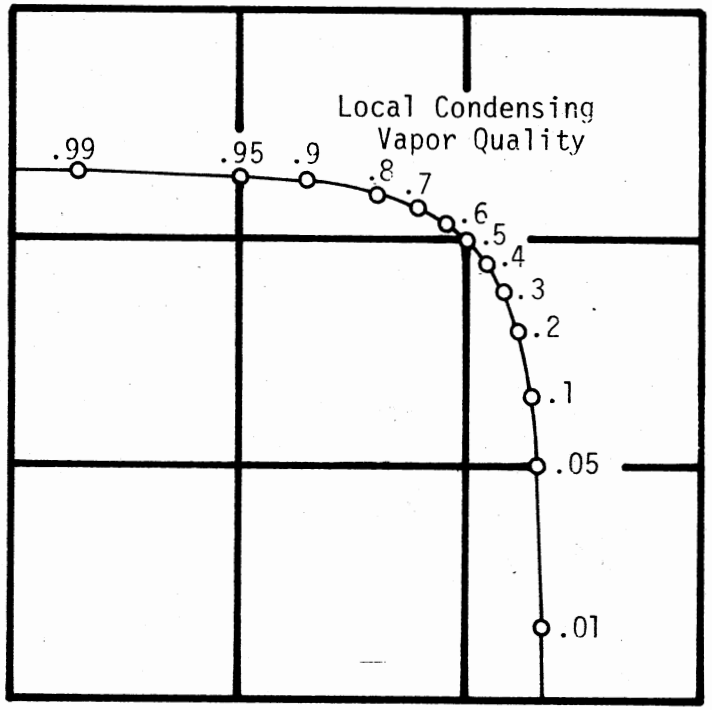

Figure 2. Overlay for Transformed Baker Map
Showing Course of Condensation

annular with mist. The Fair map (10) is generally recognized as the best for this configuration and is shown in a slightly modified form in Figure 3. The Fair map is not applicable at low condensing flow rates because it is based on the assumption of upward two-phase flow. However, if vapor shear effects are sufficient to dominate the flow behavior, the Fair map is quite useful.

Knowledge about two-phase flow patterns across tube banks, with or without baffles, is much more limited and indeed hardly extends beyond what intuition tells. In the case of two-phase flow inside horizontal tubes, wavy flow occurs mostly where the relative velocity of the vapor with respect to the liquid is about 15 feet per second. Annular flow occurs at a superficial velocity of 20 to 70 feet per second depending upon the liquid flow rate.

Driving Mechanism

The condensation of pure components is mostly a heat transfer process, wherein heat is removed from the condensing vapors across the condensate layer to the cooler wall. The driving force for the condensation process is the temperature gradient across the condensate layer.

Equipment Types Used

The condensation of pure component vapors can be carried out in a variety of heat transfer equipment. Some of the common types of condensers are shell and tube condensers, jet condensers, evaporative

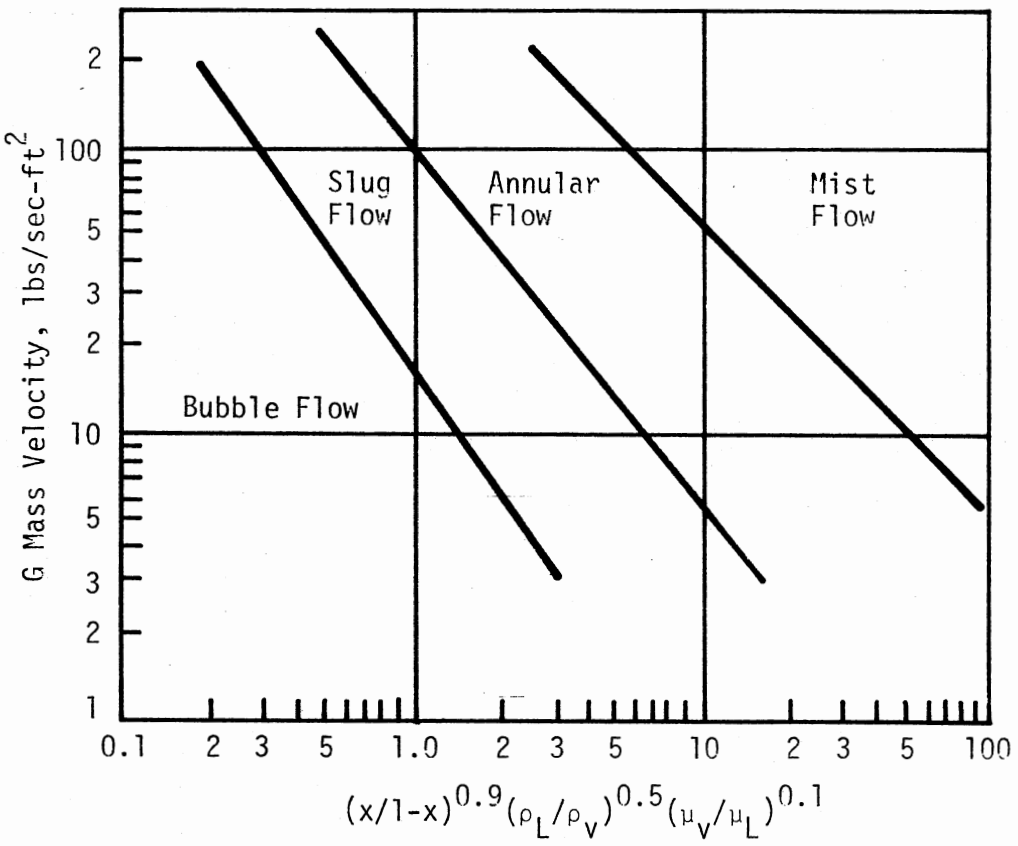

Figure 3. Modified Fair Flow Regime Map for Vertical Intube Flow

condensers, knockback condensers and air-cooled condensers. The most common type of condenser used in process plants is shell and tube condenser. A chart of the different condenser configurations that can be considered for process service and general comments about their suitability for various services is given in Table I (16). The areas of application or exclusion shown, the operating limits and the estimation of accuracy are generally true. Experience should help a great deal in the ultimate purpose of selecting and designing a condenser.

Pressure Drop and MTD Considerations

Pressure drop during the condensation process is a very important factor that has to be considered. Pressure drop for two-phase flow inside tubes is higher than that for single-phase flow. The pressure drop in condensers adversely affects the temperature difference. The greater the pressure drop the lower the condensing temperature and the greater the heat transfer area required. Very high pressure drops can lead to two-phase choking flow. In the case of the condensation of pure vapors at low pressures, the pressure drop is a critical factor in the design of condensers.

Handling of Non-Condensables

The design of a surface condenser for the condensation of vapor from a mixture of vapor with non-condensing gases presents several unusual conditions and complications in heat transmission, not encountered in the condensation of pure vapors. The properties of

TABLE I

SURVEY OF PROCESS CONDENSER CONFIGURATIONS (Ref. 16)

Shell and Tube	Subcooled Condensate	Mixed Vapor Condensation Total or Partial	Fouling or Polymerization	Corrosion	Heat Transfer Predictive Ability
Inside Tubes					
Vertical-Upward Flow	Not Applicable	Limited Range of Concentration	Not Applicable	Fair	Poor
-Downward Flow	Excellent	Excellent	Fair	Good	Good
Horizontal	Very Poor	Good in Annular Flow	Fair	Good	Good
Outside Tubes					
Vertical	Possible But Not Recommended	Good	Very Poor	Poor-alloy Shell Required	Fair
Horizontal	Not Recommended	Poor for Wide Condensing Mixtures	Very Poor	Poor	Fair
AIR COOLER					
Horizontal Tubes	Not Recommended	Good	Fair	Excellent	Good
Vertical Tubes	Excellent	Good	Fair	Excellent	Good
DIRECT CONTACT	Good	Fair	Excellent	Excellent	Very-Good (Usually Conservative)

the gas stream vary greatly as the condensation proceeds. The heat transfer coefficient of the film, the rate of vapor flow and the thermal capacity of the vapor stream decrease as the condensation proceeds. The condensation of the vapor depends upon the diffusion of the vapor through the gas; hence, mass transfer as well as heat transfer becomes important. For these reasons no method of calculating the MTD based on the terminal temperatures is applicable. The design aspects of condensers with non-condensables present are given in reference (7).

The purpose of this study is to analyze the performance of condensers for pure vapor and develop approximate design procedures for quick design of pure component condensers. Some modifications to the existing rigorous methods are also being suggested. Finally, some discussion is made about the optimization procedures to be used in the design of condensers.

CHAPTER II

ANALYSIS OF PRESSURE DROP AND MEAN TEMPERATURE DIFFERENCE RELATIONSHIP

As has been already discussed, the pressure drop in condensers adversely affects the mean temperature difference and increases the heat transfer area for a given condenser duty. Hence, an analysis of the extent to which the pressure drop affects the mean temperature difference is justified.

Variation of Saturation Temperature with Pressure Drop

The Clausius-Clapeyron equation is used to relate the variation of the saturation temperature to pressure. For a vapor entering at a pressure P_1 and saturation temperature T_1 and the condensate leaving at a pressure P_2 and saturation temperature T_2 the Clausius-Clapeyron equation simplifies to

$$\ell n \frac{P_2}{P_1} = \frac{\Delta H_v}{R} \left(\frac{1}{T_1} - \frac{1}{T_2}\right) \qquad (2\text{-}1)$$

$$\therefore \frac{P_2}{P_1} = e^{(\Delta H_v/R)\left(\frac{1}{T_1} - \frac{1}{T_2}\right)} \qquad (2\text{-}2)$$

$$\therefore \frac{P_1 - P_2}{P_1} = 1 - e^{(\Delta H_v/R)(\frac{T_2 - T_1}{T_1 T_2})} \qquad (2\text{-}3)$$

$$\therefore \frac{\Delta P}{P_1} = 1 - e^{(\Delta H_v/R)(\frac{T_2 - T_1}{T_1 T_2})} \qquad (2\text{-}4)$$

$$\therefore \ln(1 - \frac{\Delta P}{P_1}) = \frac{\Delta H_v}{R}(\frac{1}{T_1} - \frac{1}{T_2}) \qquad (2\text{-}5)$$

This can be further simplified by using the formula

$$\ln(1 - x) = - x - \frac{x^2}{2} \frac{x^3}{3} \ldots .$$

$$\therefore \ln(1 - \frac{\Delta P}{P_1}) = - \frac{\Delta P}{P_1}$$

$$\therefore - \frac{\Delta P}{P_1} = \frac{\Delta H_v}{R}(\frac{1}{T_1} - \frac{1}{T_2}) \qquad (2\text{-}6)$$

then:

$$\frac{1}{T_2} - \frac{1}{T_1} = \frac{R\Delta P}{P_1 \Delta H_v} \quad . \qquad (2\text{-}7)$$

This correlation assumes that the vapor follows the perfect gas law and the heat of vaporization ΔH_v is constant throughout the condensation process.

The saturation temperature calculated after considering the pressure drop in the condenser results in a logarithmic mean temperature difference which is lower than the LMTD calculated assuming the saturation temperature to be constant throughout the condensation

process. The effect of pressure drop on LMTD is shown on the plots made for different vapors.

$$\text{LMTD} = \frac{(T_1 - t_2) - (T_2 - t_1)}{\ell n \frac{T_1 - t_2}{T_2 - t_1}} \qquad (2\text{-}8)$$

Figure 4 shows a plot of the ratio of actual LMTD to the ideal LMTD for vapors which have high condensing temperatures, compared to the coolant. The coolant is assumed to be entering the condenser at a temperature t_1 equal to $85^{\circ}F$ and leaving the condenser at t_2 equal to $105^{\circ}F$. The overall heat transfer coefficient is assumed to be constant. Figure 5 shows a plot of the ratio for vapors which have condensing temperatures close to the temperature of the coolant medium. In both these plots the abscissa is the ratio of the pressure drop to the inlet pressure of the vapor.

The plots show that the LMTD does not vary much in the case of vapors which have high condensing temperatures compared to the coolant temperature. The higher the condensing temperature the lower is the decrease in LMTD with pressure drop. The reduction in LMTD for a pressure drop of 20 percent of the inlet pressure is less than 5 percent for a large LMTD and it is about 25 percent for small values of LMTD.

These results suggest that when the temperature difference available for condensation is small, the effect of pressure drop on LMTD becomes an important consideration. The decrease in the LMTD tends to increase the heat transfer area required for a given condensation duty. The effect may be as great as a 30 percent increase in area.

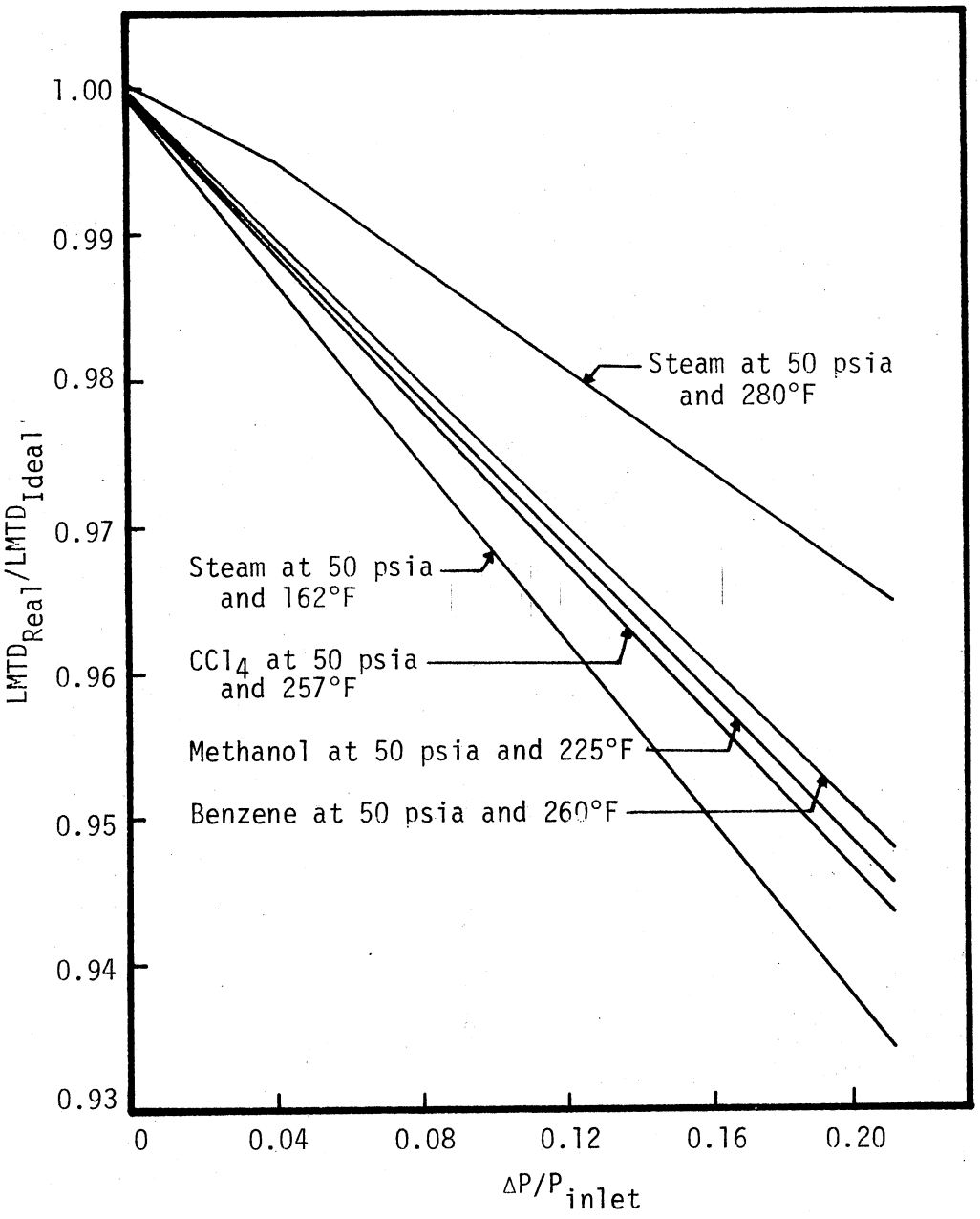

Figure 4. Variation of LMTD with Pressure Drop

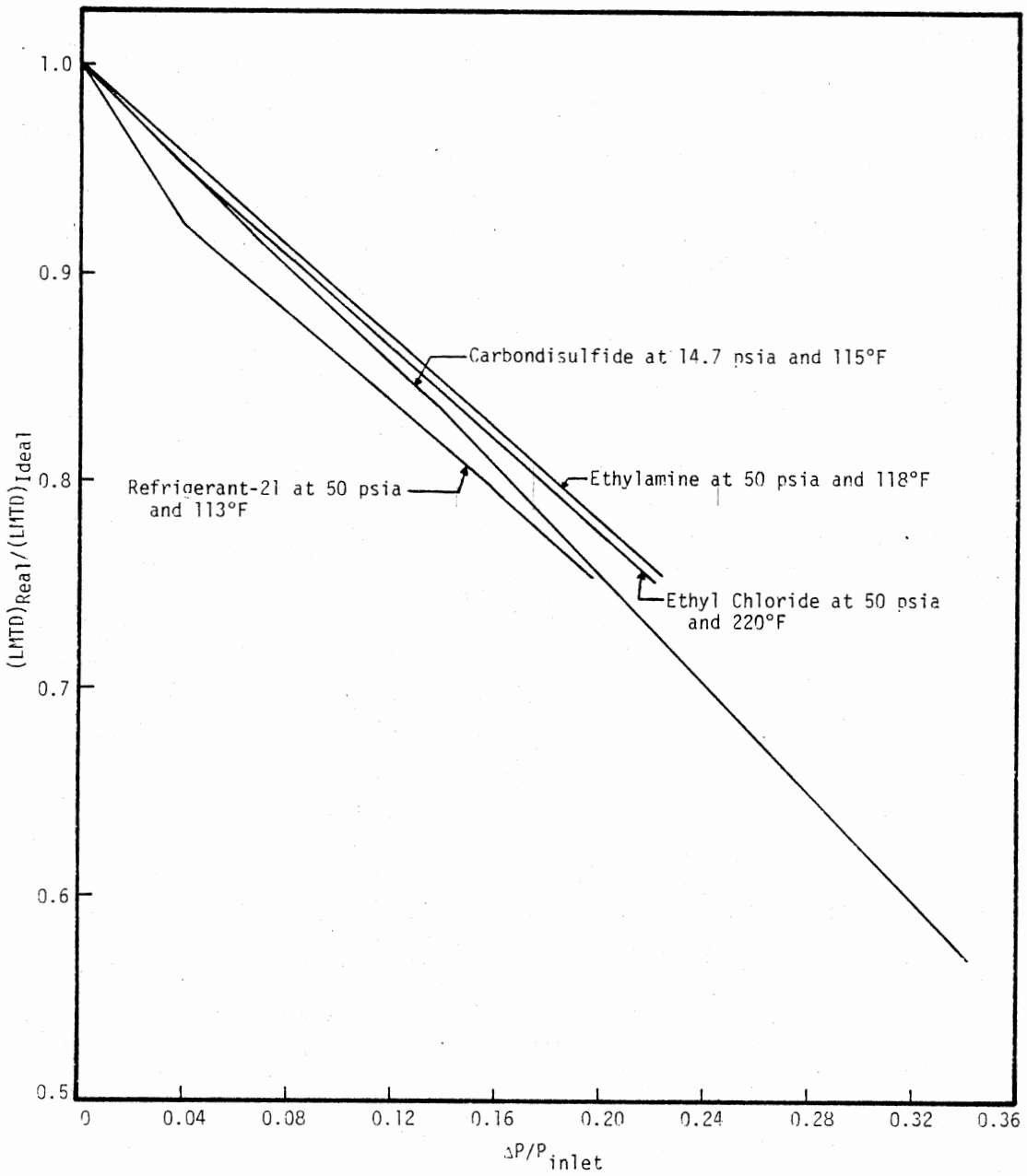

Figure 5. Variation of LMTD with Pressure Drop

CHAPTER III

EFFECT OF PRESSURE DROP ON THE FILM HEAT TRANSFER COEFFICIENT FOR CONDENSATION

The pressure drop in condensers has an effect on the condensing heat transfer coefficient. The pressure drop increases the heat transfer coefficient and thereby decreases the area required for a given condenser duty, other things remaining constant. An explanation of this effect of pressure drop follows.

The effect of pressure drop on the heat transfer coefficient for vertical intube condensation has been considered for the cases of gravity controlled-condensation and vapor shear-controlled condensation. In the case of gravity controlled-condensation, both laminar flow and turbulent flow are considered.

Nusselt's equation (13) for laminar flow gravity controlled condensation on a vertical surface is

$$h_c = 0.943 \left[\frac{K_\ell^3 \rho_\ell (\rho_\ell - \rho_g) g}{L \mu_\ell (T_s - T_w)} \right]^{1/4} \qquad (3\text{-}1)$$

As can be seen from this equation, for a given length and a given set of fluid properties, as the saturation temperature decreases h_c increases

assuming the wall temperature is constant. As discussed in the previous chapter the saturation temperature decreases with increasing pressure drop. Hence, the heat transfer coefficient increases with increasing pressure drop. The effect of pressure drop on the heat transfer coefficient for laminar flow has been shown in Figure 6. The ordinate is the ratio of h_c calculated at mean saturation temperature (average of inlet and outlet saturation temperatures) to the h_c calculated at inlet saturation temperature. The abscissa is the ratio of the pressure drop to the inlet absolute pressure. The wall temperature is assumed to be constant at $150^{o}F$ for the cases of benzene and steam condensation and $100^{o}F$ for the cases of condensation of ethyl chloride and Refrigerant-21. The effect of pressure drop is found to be large when the difference $T_s - T_w$ is large. However, the effect of pressure drop on the mean heat transfer coefficient is much greater for vapor shear controlled condensation.

In the case of turbulent flow condensation, the Colburn equation (6) is applicable. A curve fitted form of the Colburn equation is

$$h_c = 0.011 \left[\frac{K_\ell^{\,3} (\rho_\ell - \rho_g) g}{\mu_\ell^{\,2}} \right]^{1/3} Re_c^{\,1/3} \sqrt[4]{Pr_\ell} \qquad (3\text{-}2)$$

where

$$Re_c = \frac{DG(1-x)}{\mu_\ell^{\,2}} \quad \text{and} \quad Pr_\ell = \left(\frac{C_p \mu}{K} \right)_\ell \qquad (3\text{-}3)$$

Based upon the Colburn equation (3-2) the effect of pressure drop on the heat transfer coefficient has been shown in Figure 7. The ordinate in this figure is the ratio of heat transfer coefficient at any pressure drop to the heat transfer coefficient at a unit pressure drop.

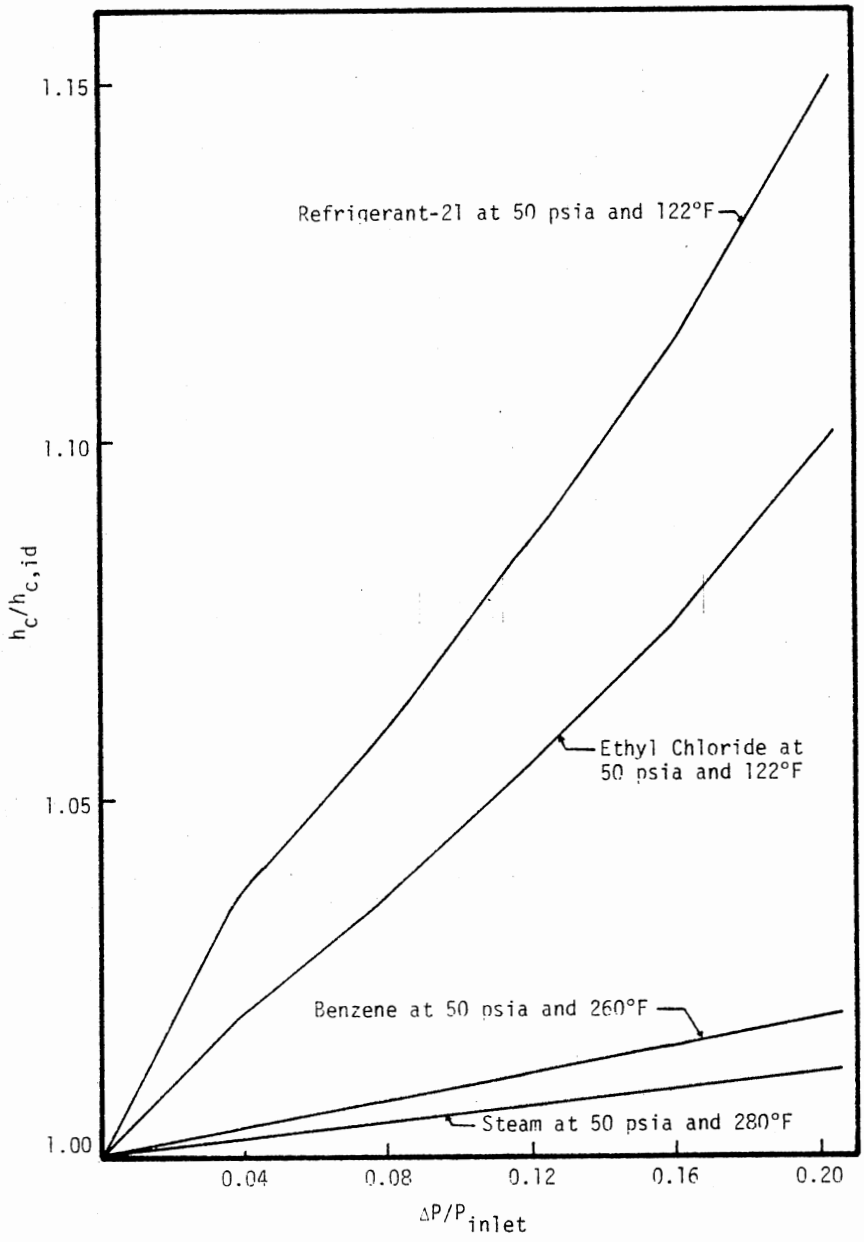

Figure 6. Effect of Pressure Drop on Heat Transfer Coefficient for Laminar Flow Conditions

Here again, the h_c increases with increasing pressure drop.

In the case of vapor shear controlled intube condensation, the Boyko-Kruzhilin correlation (5) can be used. For total condensation from a dry saturated vapor this correlation is

$$\frac{h_c D_i}{K_\ell} = 0.024 \left(\frac{D_i G_T}{\mu_\ell}\right)^{0.8} Pr_\ell^{0.43} \left[\frac{1 + \sqrt{\rho_\ell/\rho_g}}{2}\right] \qquad (3\text{-}4)$$

The effect of pressure drop on h_c in this case is shown in Figure 7. There is a large increase in h_c as the pressure drop is increased.

As can be seen from this analysis, the increase in heat transfer coefficient with increasing pressure drop, is insiginificant for laminar flow gravity controlled condensation. In this case, it is suggested that the designer pay more attention to the effect of ΔP on LMTD than on h_c. In the case of turbulent flow gravity controlled condensation, the increase in h_c with increasing ΔP is significant but the increase in h_c for vapor shear controlled condensation is very high.

Vapor shear-controlled condensation occurs at high condensing loads and vapor velocities. The heat transfer coefficient calculated itself gives an indication whether vapor shear has any effect on the condensation process. Figure 7 shows a graph of h_c at any pressure drop to h_c at a unit pressure drop against pressure drop. As can be seen from this graph the heat transfer coefficients are very high in cases of vapor shear controlled condensation.

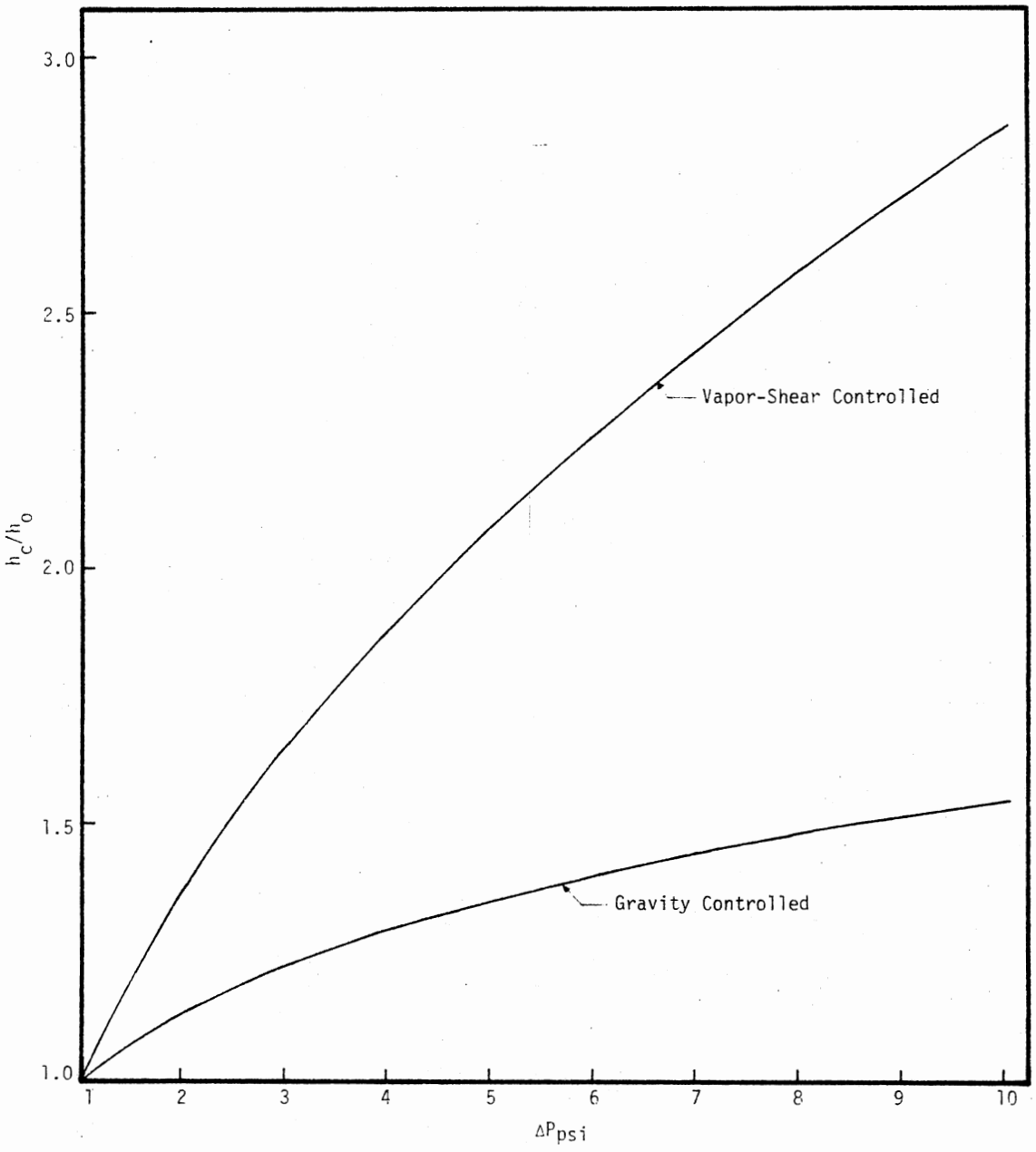

Figure 7. Effect of Pressure Drop on Heat Transfer Coefficient

CHAPTER IV

RAPID ESTIMATION OF ΔP

As has been already discussed, the pressure drop in condensers is an important aspect of the design of condensers. The calculations of two-phase flow pressure drop and heat transfer are generally much less precise than for single phase flow. The methods presented in this chapter generally work well over broad ranges of conditions and applications, but more precise methods do exist for specific situations in certain parameter ranges. This chapter deals with some methods of calculating pressure drop in condensers when condensation is occurring on the tube side or on the shell side. Only the frictional pressure drop is being considered, because it forms the major portion of the total pressure drop.

Tube Side Pressure Drop

The frictional pressure gradient for two phase flow inside tubes is calculated by the Martinelli-Nelson correlation (12):

$$\left(\frac{dp}{d\ell}\right)_{f,TPf} = \Phi^2_{\ell tt} \, X_{tt}^{1.75} \left(\frac{dp}{d\ell}\right)_{f,v} \tag{4-1}$$

where:

$$X_{tt} = \left(\frac{1-x}{x}\right)\left(\frac{\rho_v}{\rho_\ell}\right)^{0.57}\left(\frac{\mu_\ell}{\mu_v}\right)^{0.11} \tag{4-2}$$

and

$$\left(\frac{dp}{d\ell}\right)_{f,v} = \frac{-2f_v G_v^2}{g_v \rho_v D} \tag{4.2}$$

$\Phi^2_{\ell tt}$ is read from Figure 8 for the value of $\sqrt{\chi_{tt}}$ calculated.

When the above calculations are based on the liquid phase we have the following equations (16)

$$\left(\frac{dp}{d\ell}\right)_{f,TPF} = \Phi^2_{\ell tt} \left(\frac{dp}{d\ell}\right)_{f,\ell} \tag{4.4}$$

$$\left(\frac{dp}{d\ell}\right)_{f,\ell} = \frac{2f_\ell G_\ell^2}{g_c \rho_\ell D} \tag{4.5}$$

f_ℓ or f_v can be read from Figure 9.

If Re_ℓ is greater than 2100, equations 4.4 and 4.5 are used. If Re_ℓ is less than 2100 and Re_v is greater than 2100, equations 4.1 and 4.3 are used (16). If both Re_ℓ and Re_v are less than 2100, an approximate value may be obtained using the laminar flow friction factor equation for either phase

$$f_\ell \text{ or } f_v = \frac{16}{Re_\ell \text{ or } Re_v} \tag{4.6}$$

However, in this case, the pressure drop will be so low as to be unimportant.

The total frictional pressure drop from one end of the condenser to the other end must be found by integration of equations 4.1 or 4.4 over the quality range

$$\Delta P_{TPF} = \int_{x_1}^{x_o} \left(\frac{dp}{d\ell}\right)_{f,TPf} \left[1/\left(\frac{dx}{d\ell}\right)\right] dx \tag{4.7}$$

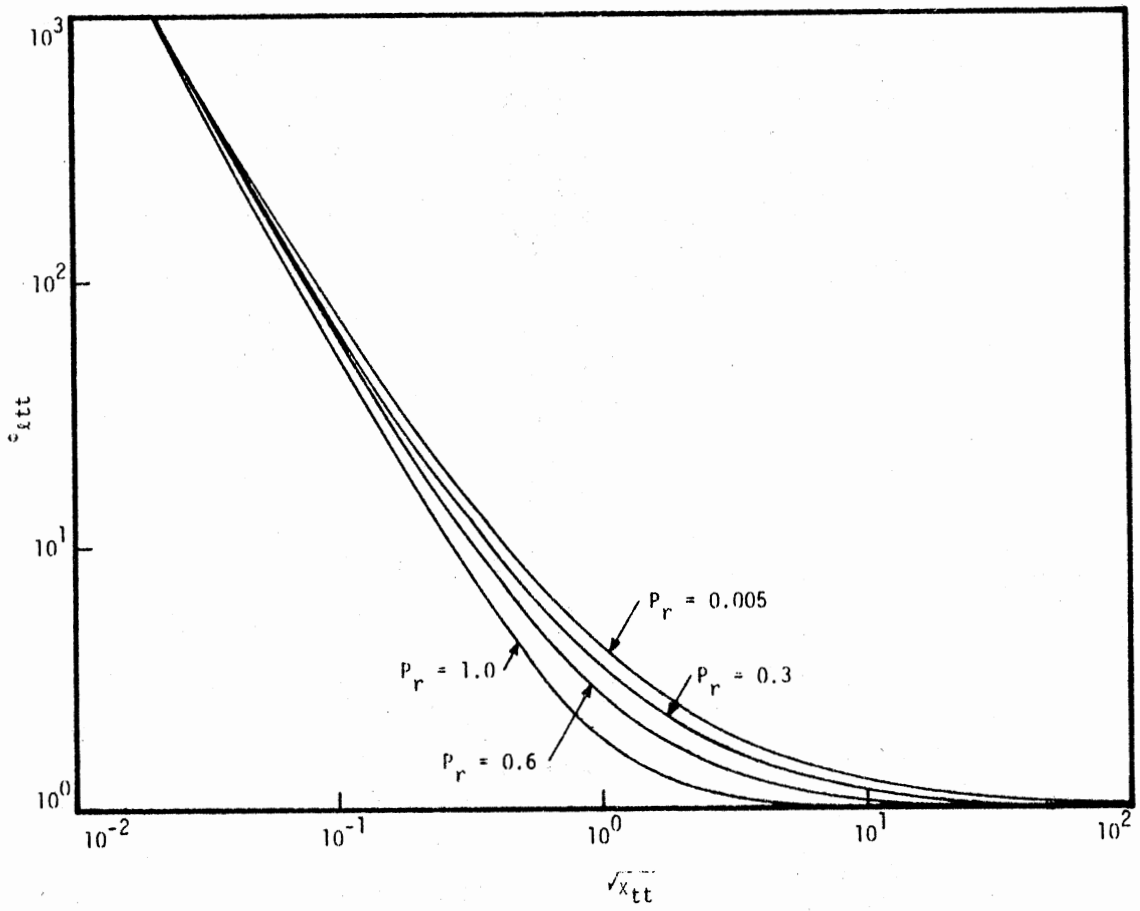

Figure 8. Correlation of $\Phi^2_{\ell tt}$ as a Function of $\sqrt{X_{tt}}$

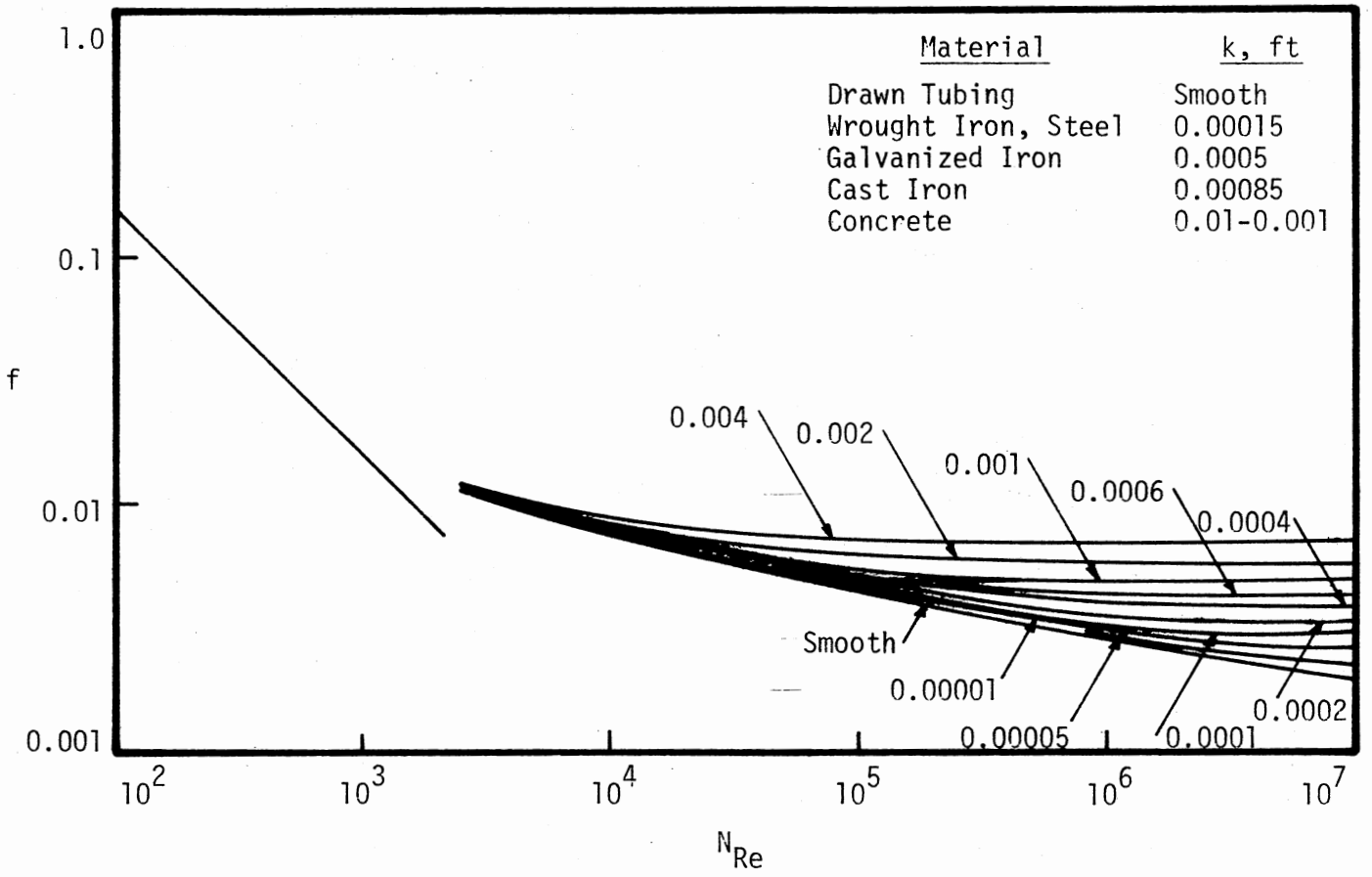

Figure 9. Fanning Friction Factors Chart for Flow Through Cylindrical Conduits

The exact numerical evaluation of this integral is a rather tedious trial and error procedure, even on a computer, because the properties and the local quality depend upon the local pressure and the integrated heat transfer rate implicity. For a condenser, however, one is usually concerned with complete condensation ($x_i = 1$; $x_o = 0$) and a very nearly linear condensation rate, ($dx/d\ell = 1/L$). Then a good approximation to ΔP_{TPF} is obtained by a "pseudo-simpson" rule (16):

$$\Delta P_{TPF} = \left\{ \frac{25}{96} \left[\left(\frac{dp}{d\ell}\right)_{\substack{TPF \\ x=0.1}} + \left(\frac{dp}{d\ell}\right)_{\substack{TPF \\ x=0.9}} \right] + \frac{23}{48} \left(\frac{dp}{d\ell}\right)_{\substack{TPF \\ x=0.5}} \right\} \Delta L \qquad (4.8)$$

The method of calculating the pressure drop on the tube side is still a rather tedious method. If a designer is doing very preliminary calculations, he need not go through this long procedure. The remaining part of the section deals with a simpler and quicker method of predicting the tube side pressure drop.

The tube side pressure drop can be predicted by the equation

$$\Delta P_{TPF} = \overline{\Phi^2}_{\ell tt} \left(\frac{4fG^2L}{2g_c D\rho}\right) \qquad 4.9$$

where:

$\overline{\Phi^2}_{\ell tt}$ is read from Figure 10, 11, 12 or 13, for the required exit vapor quality and the appropriate parameter R_1 defined by

$$R_1 = \left(\frac{\rho_v}{\rho_\ell}\right)^{0.57} \left(\frac{\mu_\ell}{\mu_v}\right)^{0.11} \qquad 4.10$$

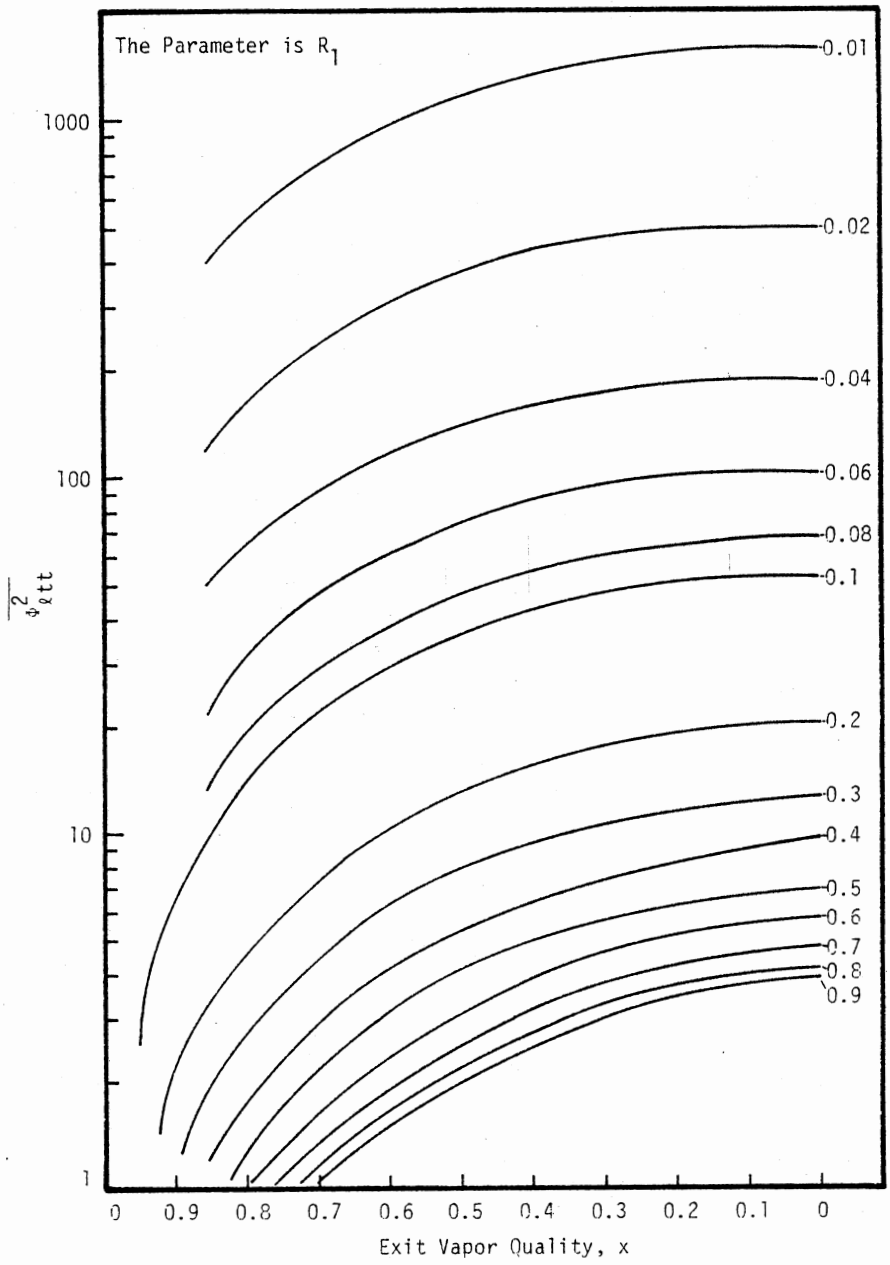

Figure 10. Multiplying Factors for Liquid Phase

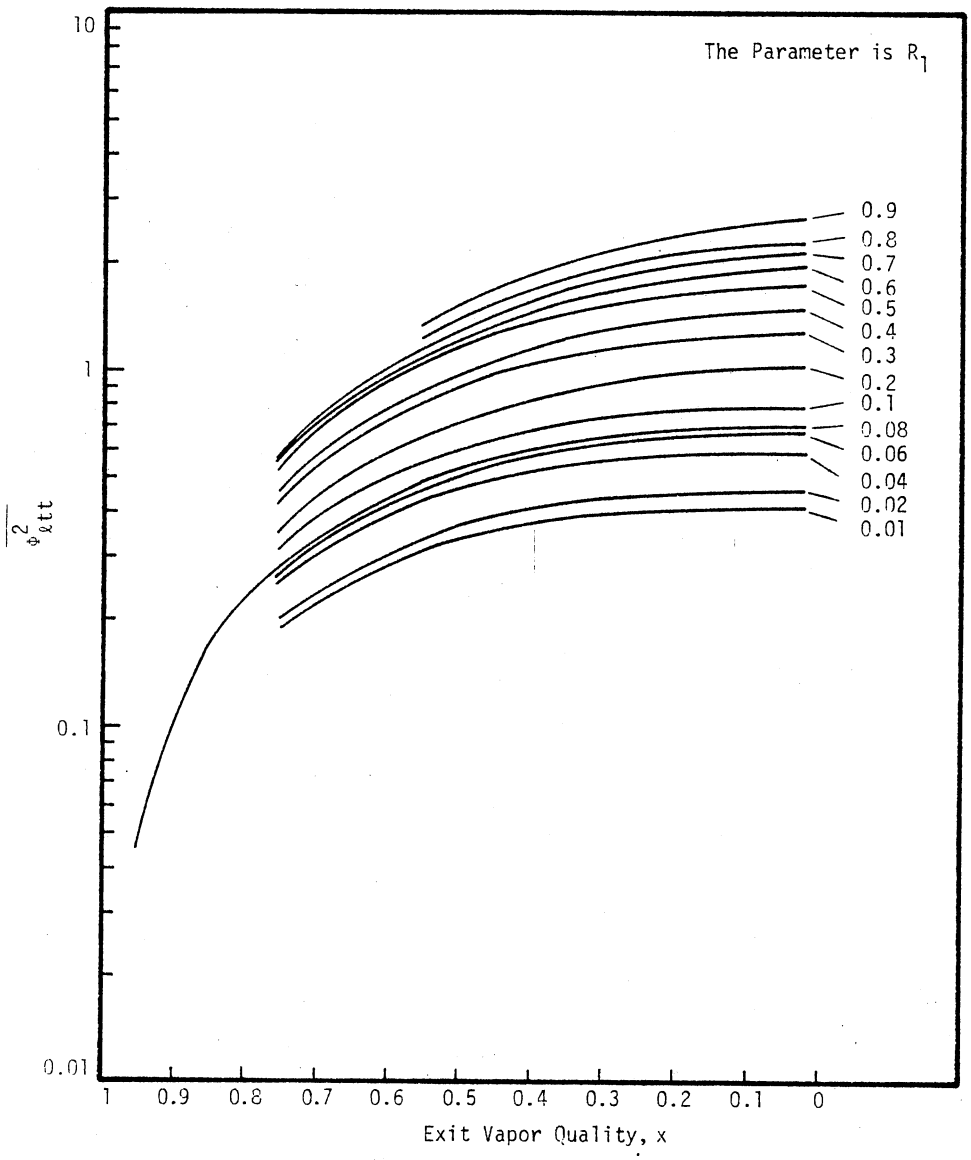

Figure 11. Multiplying Factors for Vapor Phase

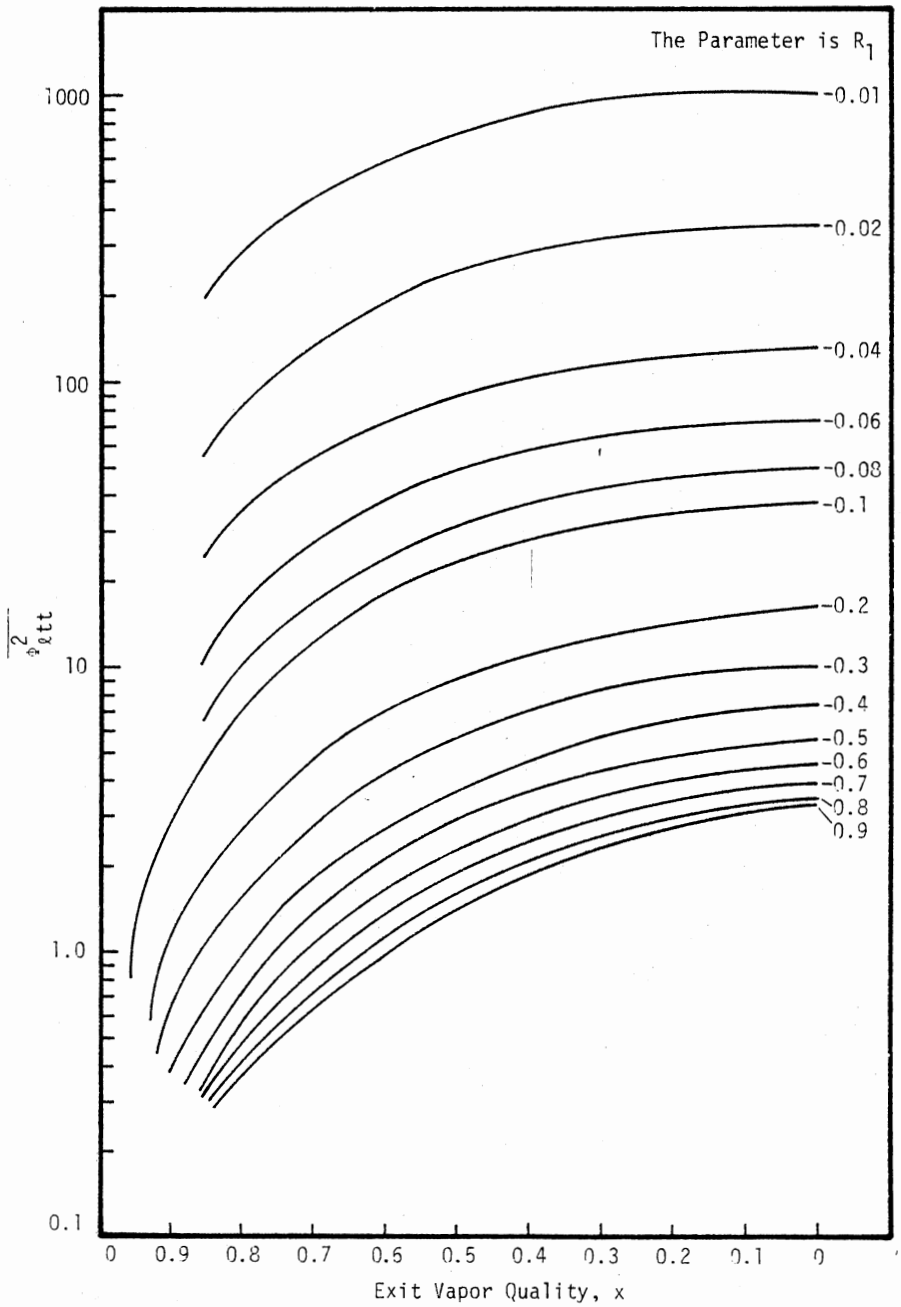

Figure 12. Multiplying Factors for Liquid Phase with Varying Friction Factor

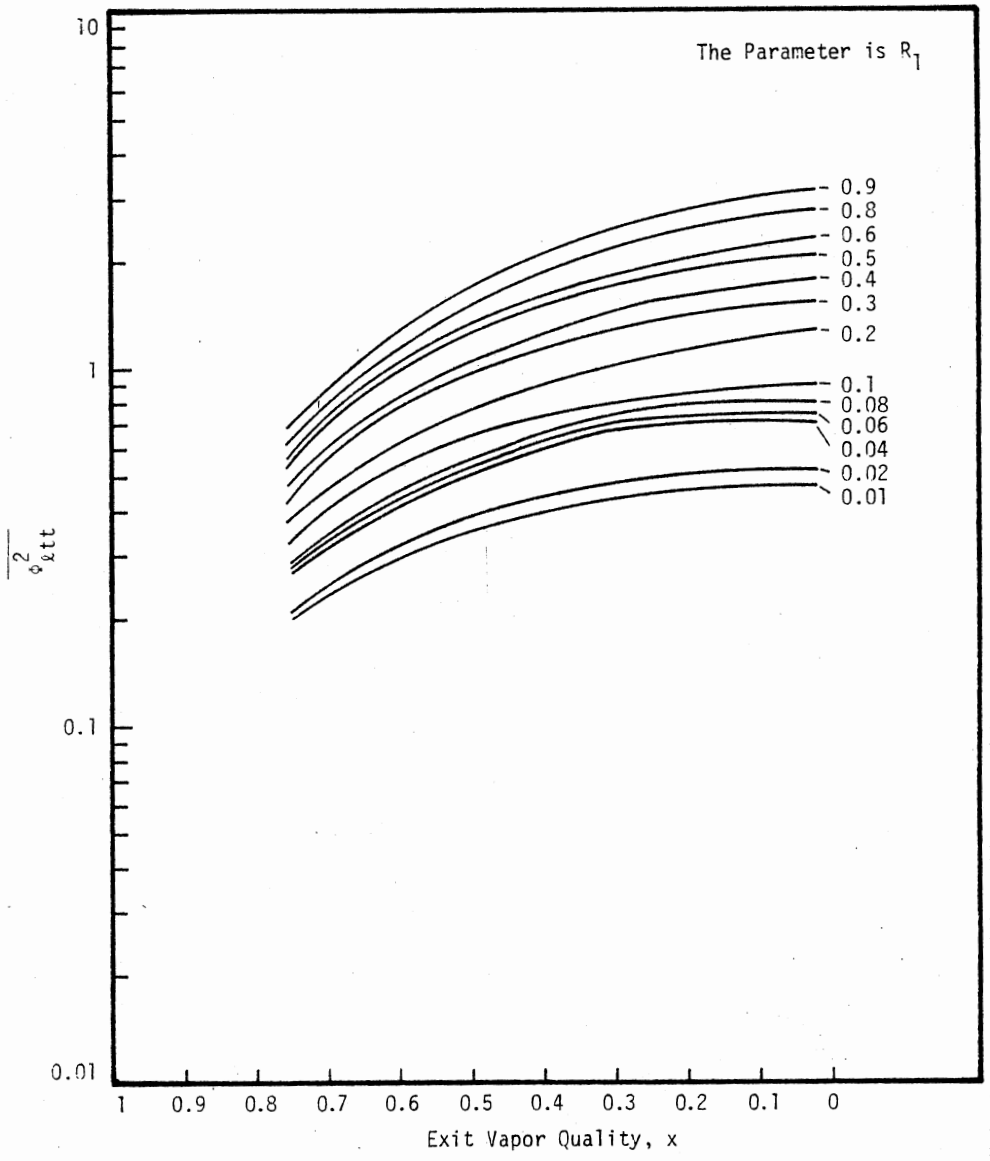

Figure 13. Multiplying Factors for Vapor Phase with Varying Friction Factor

The development of these figures is given in Appendix A. The proper figure to be used depends upon the phase on which the calculations are based and if that particular phase is in turbulent region or not. If the calculations are based on the liquid phase, Figure 10 or 12 is used. Figure 12 is used when the liquid phase is expected to be in turbulent flow conditions and the equations to be used is

$$\Delta P_{TPF} = \frac{0.156\mu_{\ell}^{0.25} G^{1.75} L}{D^{1.25} \rho_{\ell} g_c} \overline{\Phi^2}_{\ell tt} \qquad (4.11)$$

otherwise Figure 10 is to be used and f_{ℓ} is read from Figure 9. If the calculations are based on the vapor phase and this phase expected to be in the turbulent region, Figure 13 is used and the equation to be used is

$$\Delta P_{TPF} = \frac{0.156\mu_{v}^{0.25} G^{1.75} L}{D^{1.25} \rho_{v} g_c} \overline{\Phi^2}_{\ell tt} \qquad (4.12)$$

othewise Figure 11 is to be used and f_v is read from Figure 9 for the calculated Re_v. The criterion for selecting the phase for calculations depends upon the Reynolds number of each phase as discussed earlier.

Hence, the steps involved in calculating the tube side pressure drop in condensers are

1. calculate R_1 for the substance condensing by equation (4.10).
2. calculate Re_v and Re_{ℓ}. Select the phase on which the calculations are to be based and hence, the proper figure for reading factor $\overline{\Phi^2}_{\ell tt}$.

3. Read $\overline{\Phi^2}_{\ell tt}$ from the appropriate figure corresponding to the exit vapor quality.

4. Use the appropriate equation 4.9, 4.11 or 4.12 to calculate the two-phase pressure drop.

This short-cut method predicts pressure drops which are very close to the pressure drops predicted by the equations of Martinelli and Nelson.

Prediction of Shell-Side Pressure Drop

There has not been much work done on two-phase flow across banks of tubes. Diehl and Unruh (9) did some experiments on two-phase flow across banks of horizontal tubes for different tube layouts. Figure 14 shows the plot of $\frac{\Delta P_{TPF}}{\Delta P_g}$ against $\frac{(LVF)\rho_\ell}{\rho_g}$. This graph was developed from the experiments on the condensation of pure vapors across banks of horizontal tubes. This graph can be used to predict the pressure drop for condensation across banks of tubes by using pointwise calculations.

Figure 15 shows a plot of multiplying factor $\overline{\Phi^2}_{\ell tt,CF}$ against the exit vapor quality x. This graph has been developed from Figure 14 and the development is shown in Appendix B. The shell side pressure drop can be calculated by the equation

$$\Delta P_{TPF} = \left[\Delta P_{g,CF} R_{ST,CF} \overline{\Phi^2}_{\ell tt,CF}\right](N_{b+1}) + \left[\Delta P_{g,w} R_{ST,w} \overline{\Phi^2}_{\ell tt}\right] N_b \qquad (4.13)$$

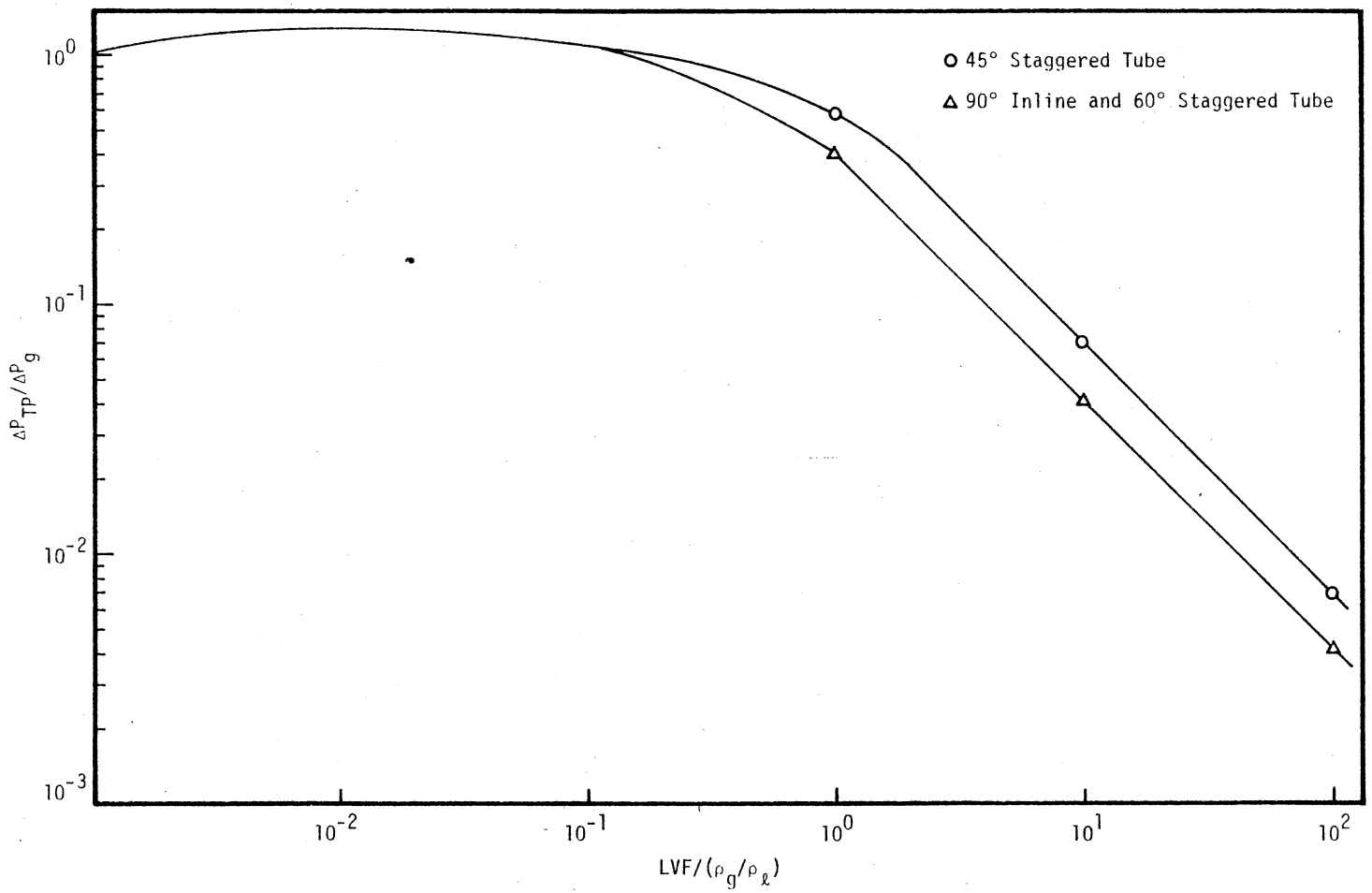

Figure 14. Two Phase Pressure Drop Correlation for Turbulent Horizontal Flow Through Tube Banks

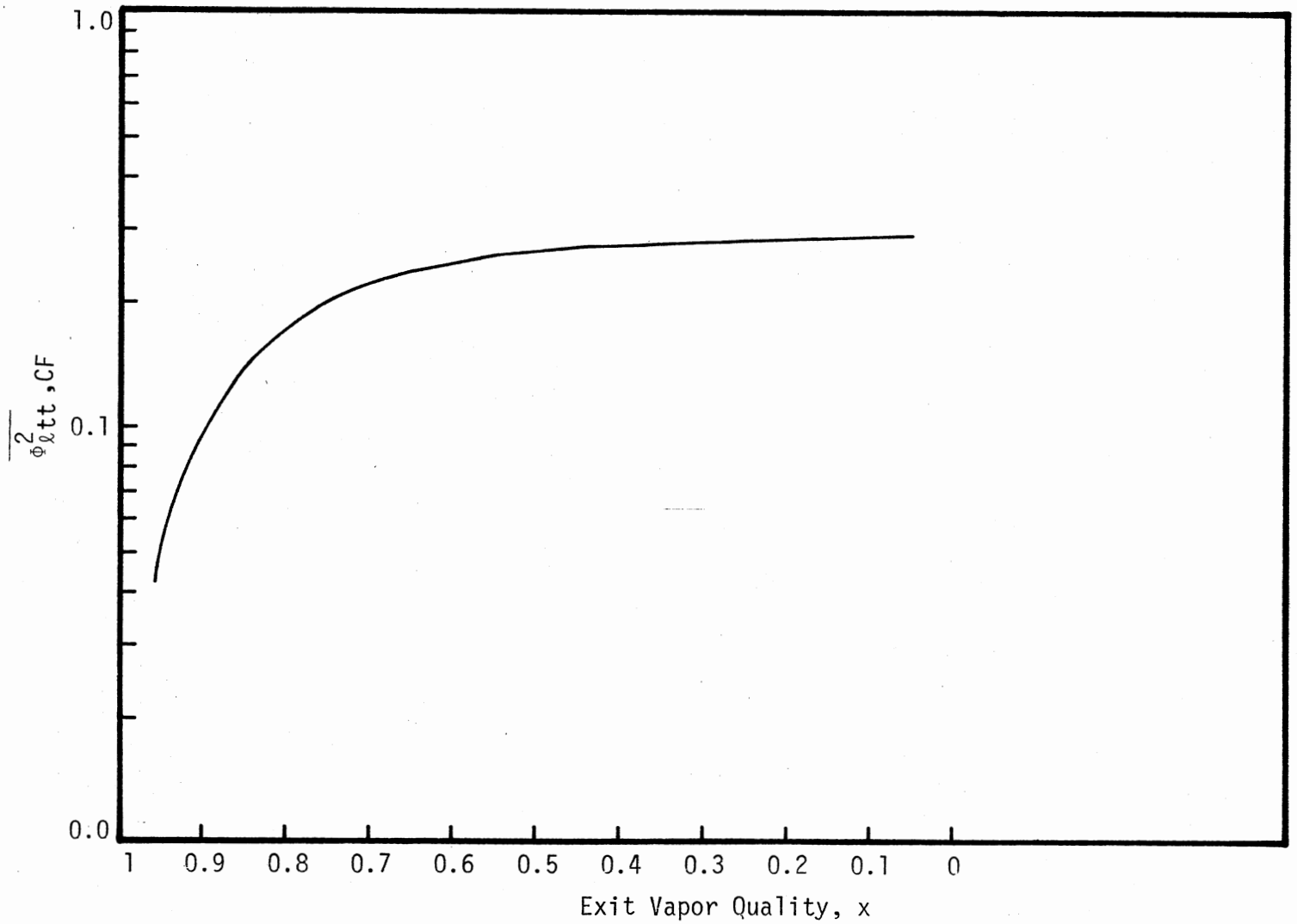

Figure 15. Multiplying Factor for Shell Side

This equation can be used in conjunction with the Delaware method (16) for design of shell and tube heat exchangers. The Delaware method is discussed below. The shell side geometry data known are d_o, tube geometrical arrangement, D_i, D_{otl}, l, l_c, l_s and N_{ss}.

Calculation of Shell-Side Geometric Parameters

1. Number of tubes N_t is found from tube count table (16).
2. Tube pitch parallel to flow p_p, and normal to flow, p_N are found from Table V corresponding to d_o, p and tube layout selected.
3. $N_c = \dfrac{D_i\left[1-2\left(\frac{l_c}{D_i}\right)\right]}{p_p}$
4. F_c is read from Figure 16 as a function of baffle cut $\left[\left(\frac{l_c}{D_i}\right)(100\%)\right]$, and shell diameter D_i.
5. $N_{cw} = \dfrac{0.8 l_c}{p_p}$
6. $N_b = \dfrac{12l}{l_s} - 1$
7. $S_m = l_s\left[D_i - D_{otl} + \left(\frac{D_{otl}-d_o}{p_N}\right)(p-d_o)\right]$, in.^{2} for rotated and inline square layouts;

   $S_m = l_s\left[D_i - D_{otl} + \left(\frac{D_{otl}-d_o}{p}\right)(p-d_o)\right]$, in.^{2} for triangular layouts.

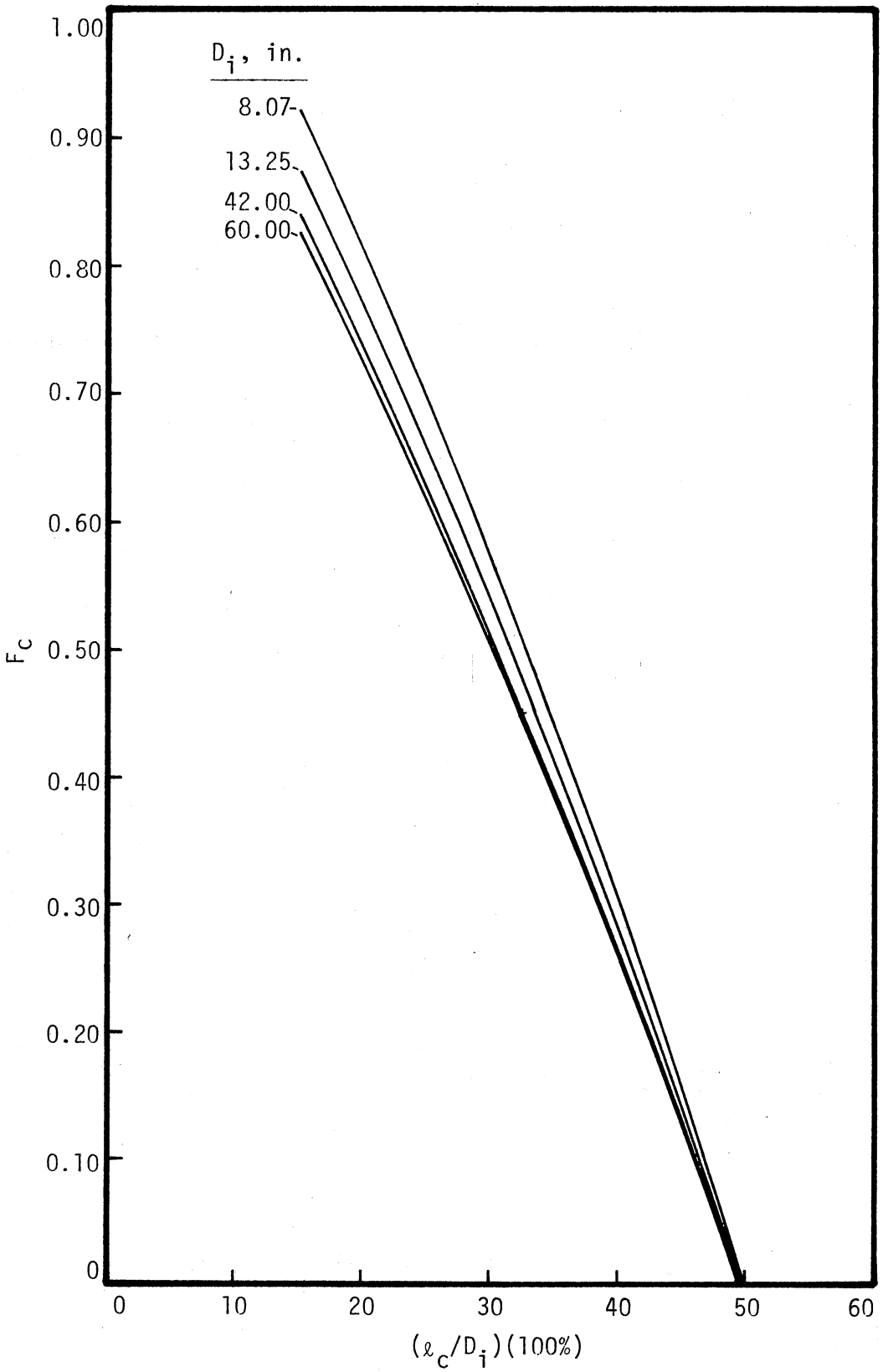

Figure 16. Estimation of Fraction of Tubes in Crossflow

8. $F_{sbp} = \frac{(D_i - D_{otl})\ell_s}{S_m}$

9. S_{tb} is calculated as follows:

   d_o = 5/8 in.: $S_{tb} = 0.0152N_t(1+F_c)$, in.^{2}

   d_o = 3/4 in.: $S_{tb} = 0.0184N_t(1+F_c)$, in.^{2}

   d_o = 1 in.: $S_{tb} = 0.0245N_t(1+F_c)$, in.^{2}

10. S_{sb} is read from Figure 17 as a function of D_i and percent baffle cut.

11. $S_w = S_{wg} - S_{wt}$

    S_{wg} is read from Figure 18A as a function of percent baffle cut and D_i

    S_{wt} is read from Figure 18B as a function of N_t and F_c.

Calculations of Correction Factors

1. R_ℓ is read from Figure 19 as a function of $(S_{sb} + S_{tb})/S_m$ with $S_{sb}/(S_{sb}+S_{tb})$ as parameter.
2. R_b is read from Figure 20 as a function of F_{sbp} and N_{ss}/N_c.

Once these calculations are made, the shell side pressure drop can be calculated by using equation (4.13)

where:

$$\Delta P_{g,CF} = 0.69 \times 10^{-6} \frac{f_i W_s^2 N_c}{\rho_s S_m^2}, \text{ lbf/in}^2 \qquad (4.14)$$

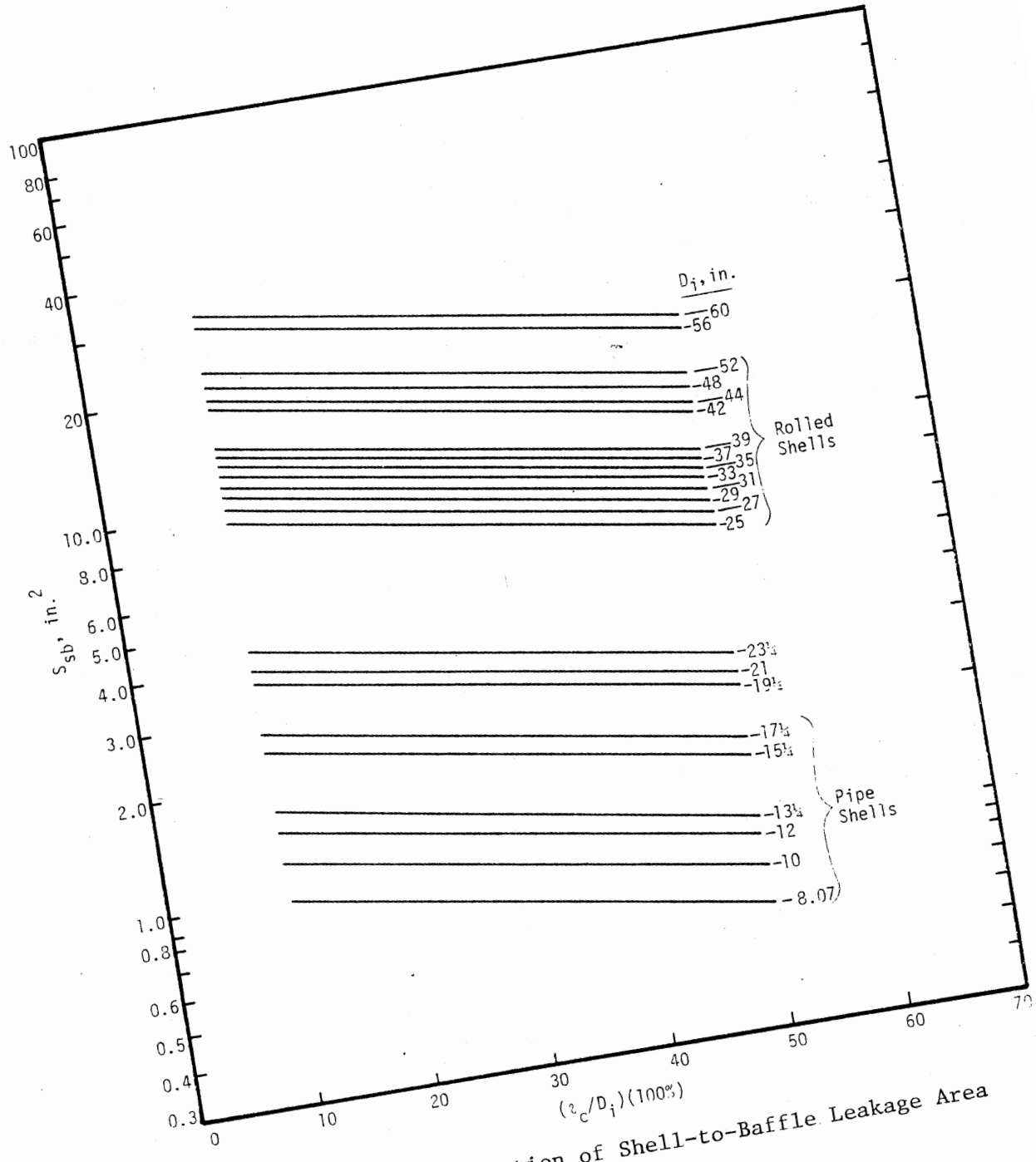

Figure 17. Estimation of Shell-to-Baffle Leakage Area

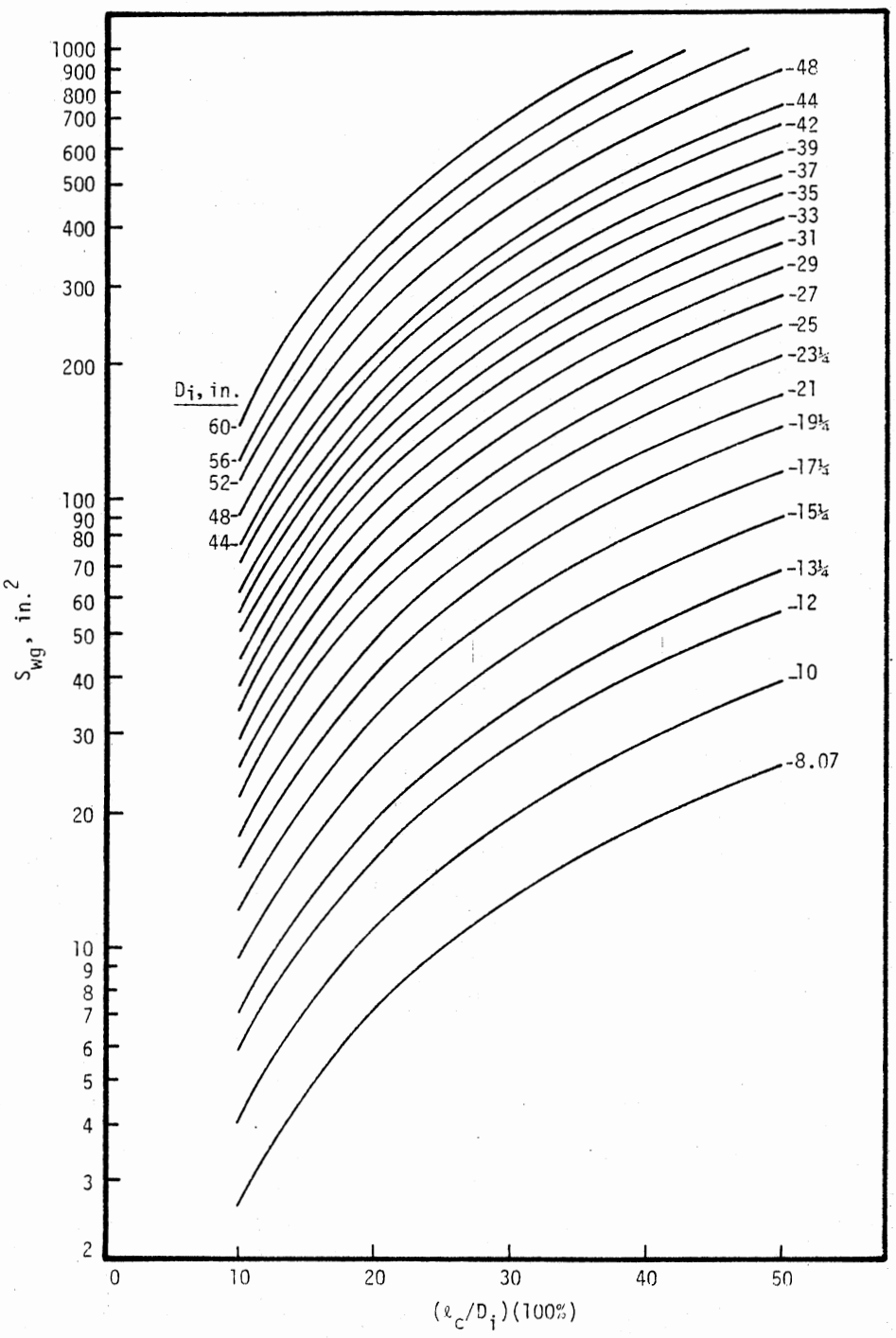

Figure 18A. Estimation of Window Crossflow Area

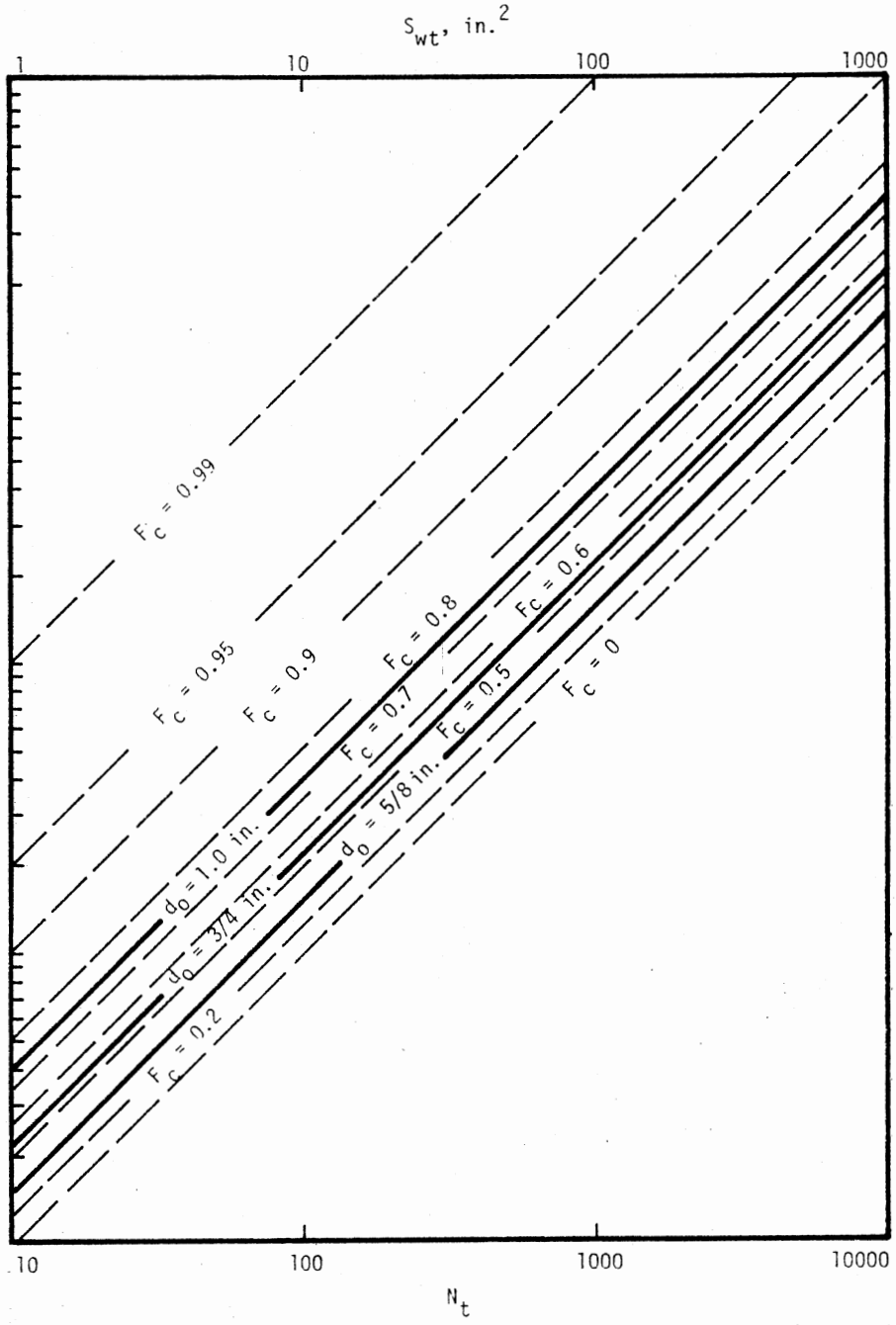

Figure 18B. Estimation of Cross-Sectional Area of Tubes in Window

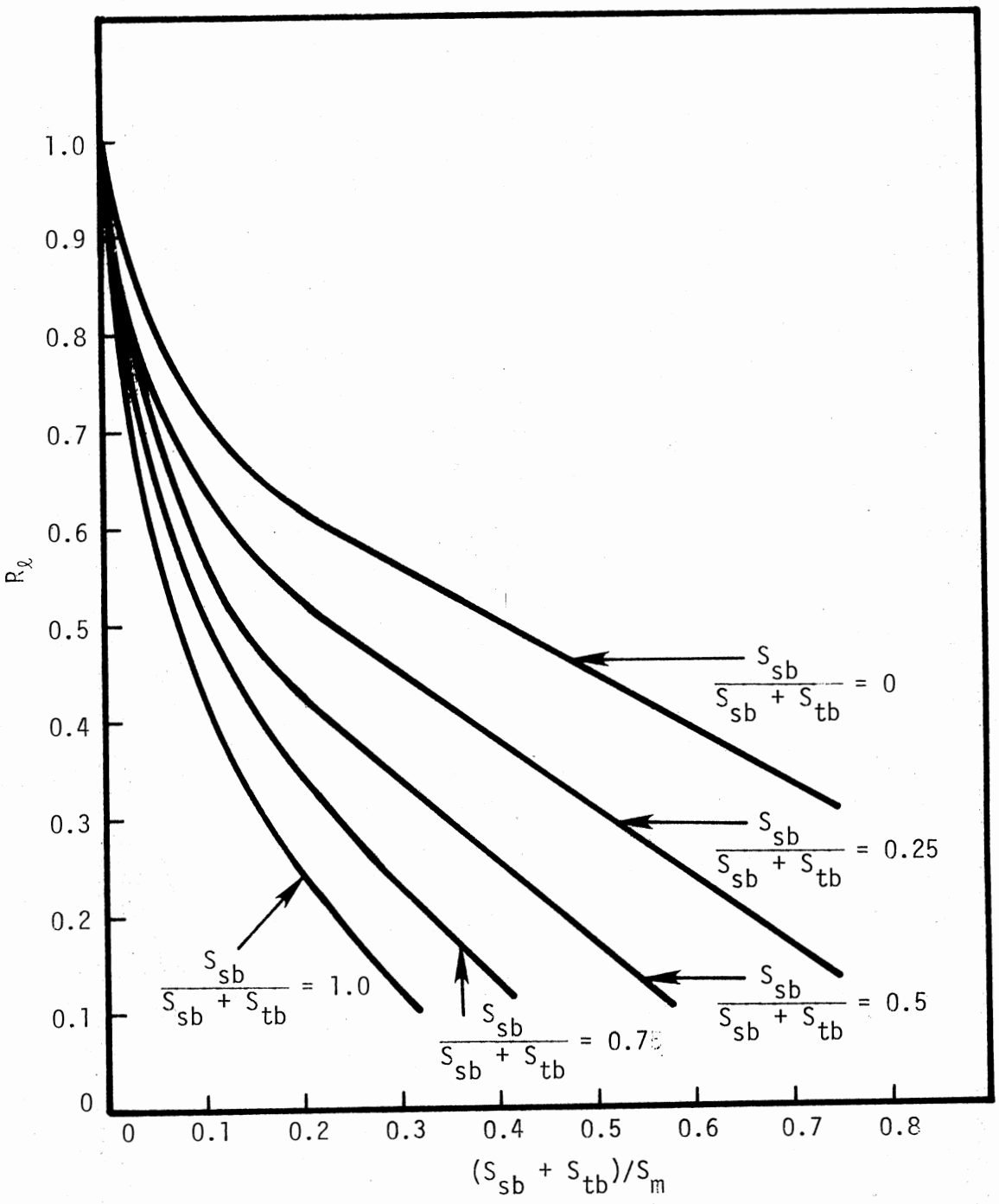

Figure 19. Correction Factor for Baffle Leakage Effect on Pressure Drop

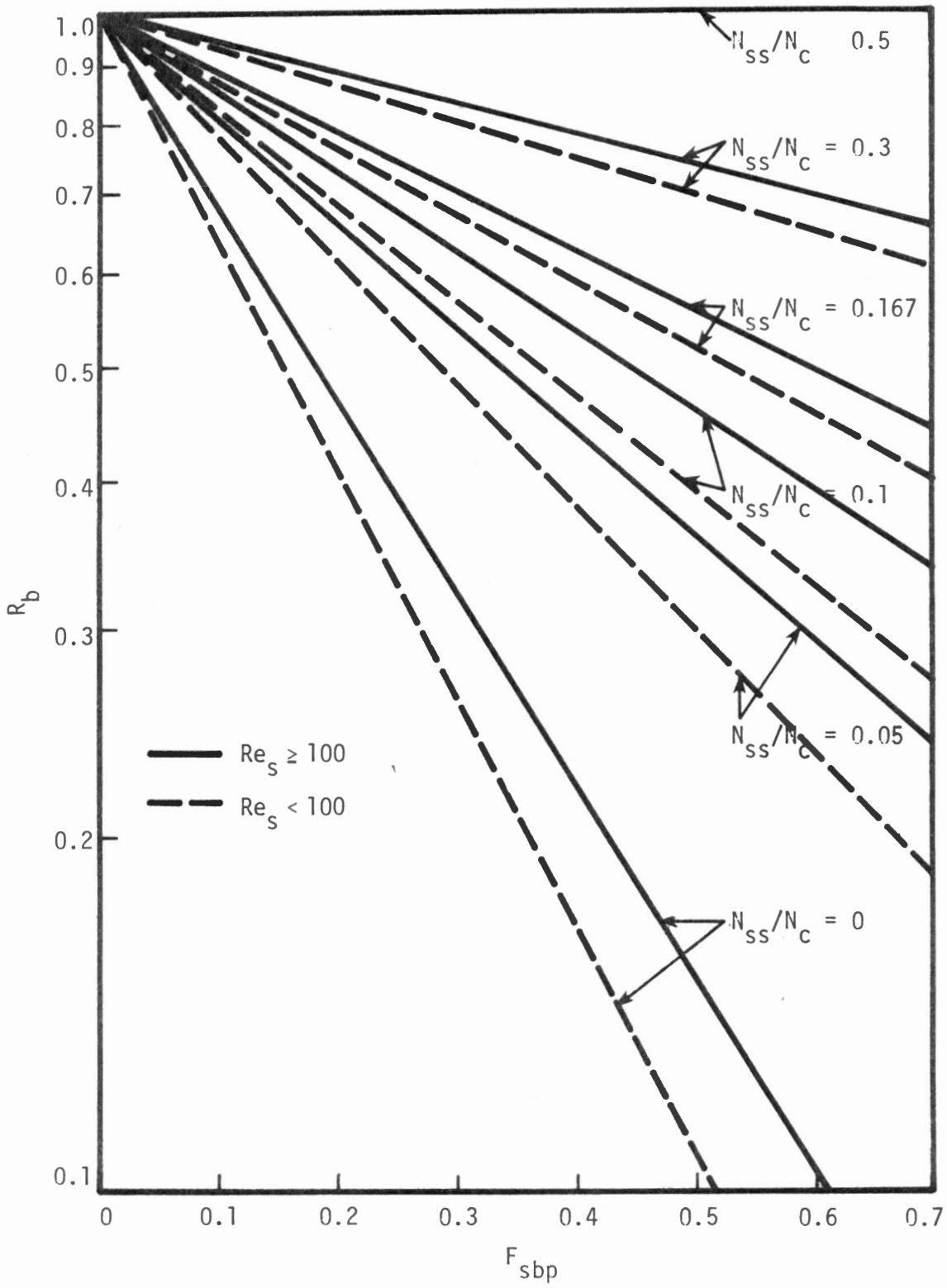

Figure 20. Correction Factor on Pressure Drop for Bypass Flow

$$\Delta P_{g,w} = 1.73 \times 10^{-7} \frac{W_s^2 (2+0.6N_{cw})}{S_m S_w \rho_s}, \text{ lbf/in}^2 \quad (4.15)$$

f_i is read from Figure 21A or 21B for the R_e calculated.

$$R_{ST,CF} = R_L x R_b \quad (4.16)$$

$$R_{ST,W} = R_L \quad (4.17)$$

$\overline{\Phi^2}_{\ell tt,CF}$ is read from Figure 15

and

$\overline{\Phi^2}_{\ell tt}$ is obtained from Figures 10, 11, 12 or 13, the proper figure chosen according to the criteria discussed earlier.

Obviously this method for prediction of shell side pressure drop is a tedious one and for preliminary calculations a quicker method could be used. The following simplified method could be used for a quick estimate of shell side pressure drop.

$$S_m = \frac{D_i c \ell_s}{p_N} \quad (4.18)$$

where c is the clearance between tubes calculated as $p-d_o$. Also, it is assumed that:

$$S_w = S_m \quad (4.19)$$

$$R_{ST,CF} = 0.45 \quad (4.20)$$

$$R_{ST,W} = 0.6 \quad (4.21)$$

$$f_i = 0.1 \text{ to } 0.12 \quad (4.22)$$

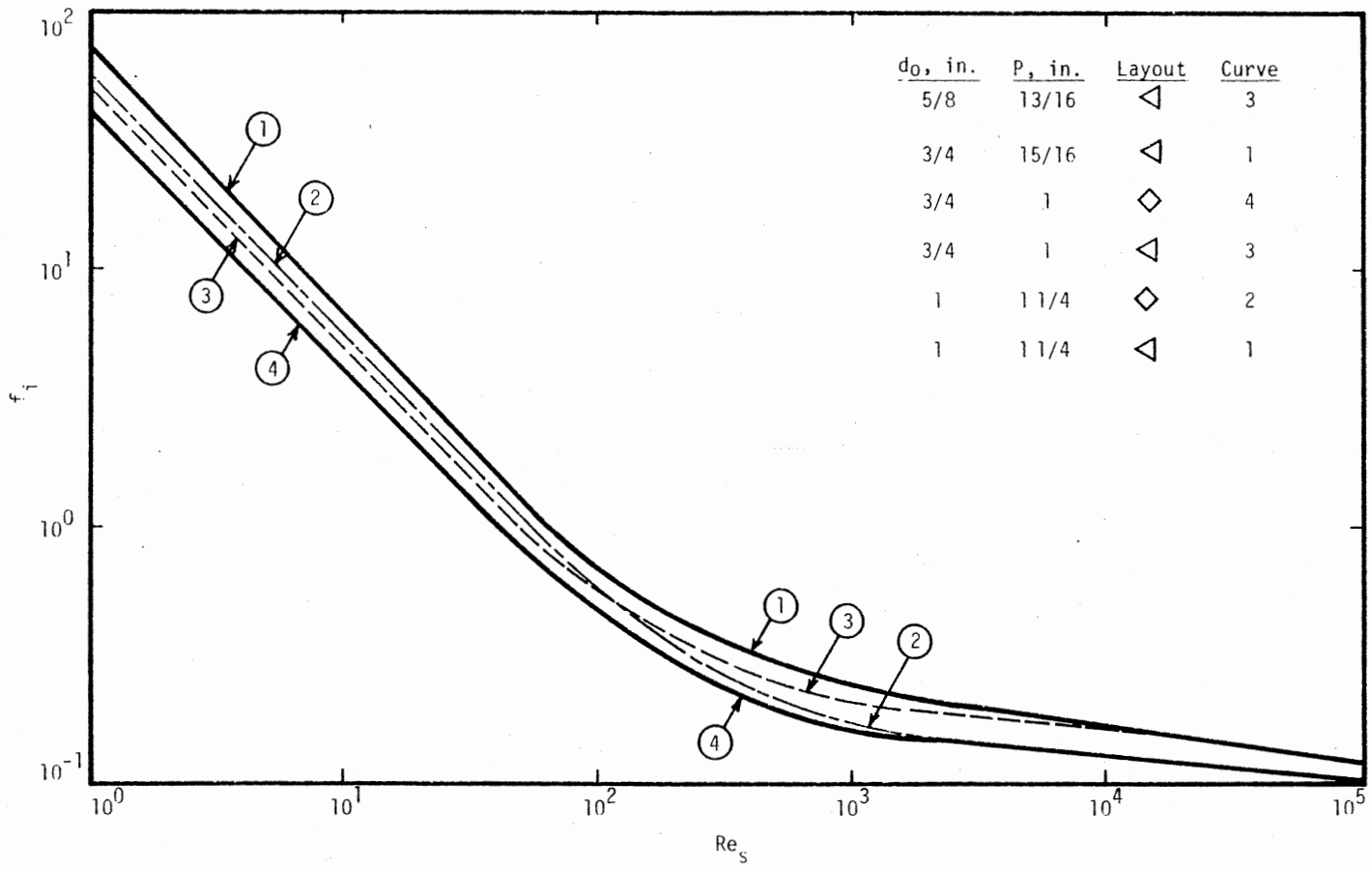

Figure 21A. Correlation of Friction Factors for Ideal Tube Banks

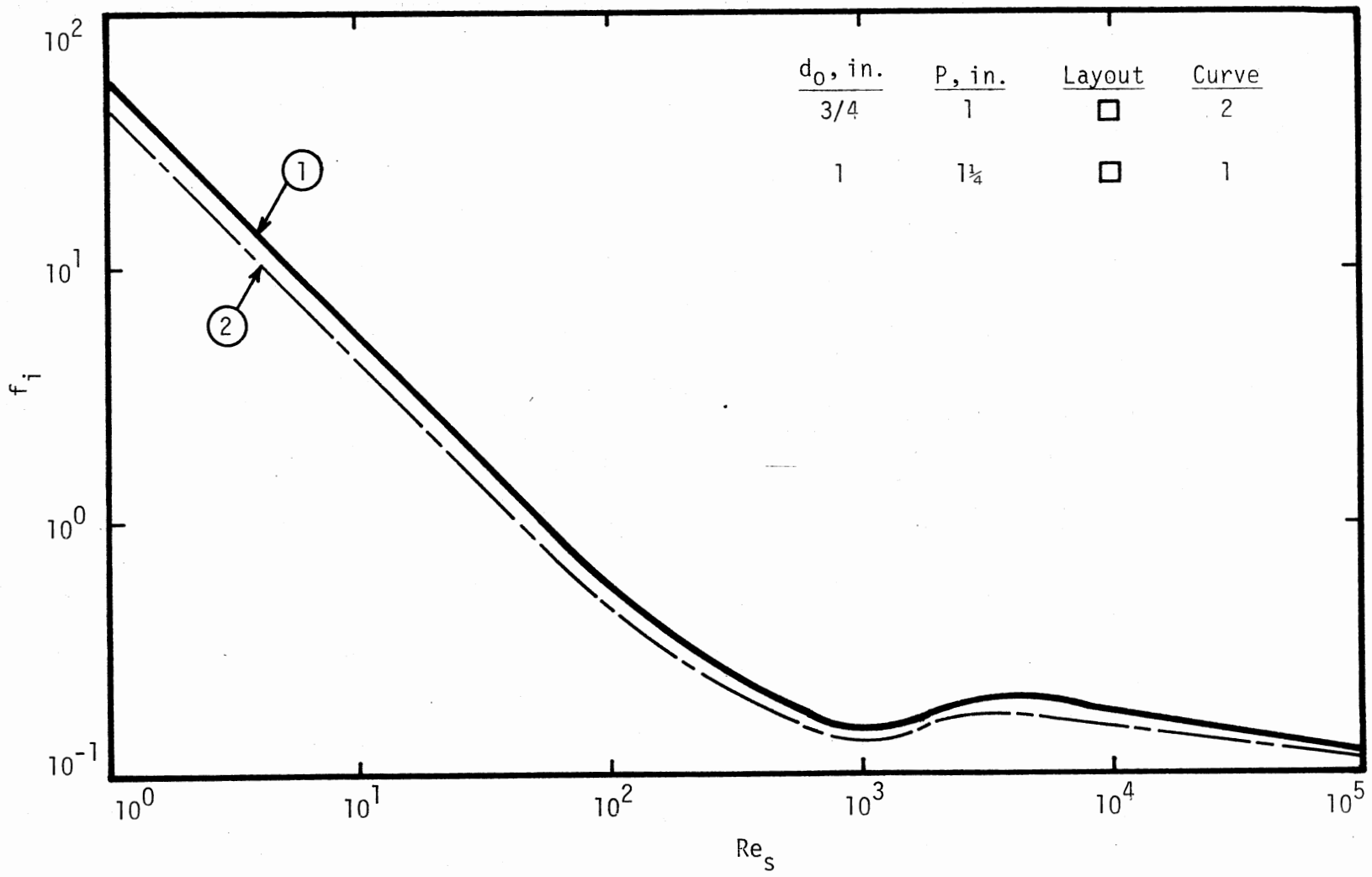

Figure 21B. Correlation of Friction Factors for Ideal Tube Banks

The use of these equations gives a quick estimate of the shell side pressure drop. These equations predict pressure drops which are adequate for preliminary estimates.

The methods outlined in this chapter have not been checked for accuracy against experimental data points. It is expected that they will give a reasonably good prediction of pressure drops.

CHAPTER V

RAPID ESTIMATION OF HEAT TRANSFER COEFFICIENT

This chapter deals with the different methods available for calculating the film heat transfer coefficient for condensation. Typical heat transfer coefficients have been tabulated and the range of overall coefficients for different services have been given.

Calculation of the Condensate Film Coefficient

Inside Vertical Tubes

For the calculation of the condensing coefficient in vertical tubes there are three cases which must be considered. For the case of low tube loadings and condensate flow rates, the condensate film flow is gravity-dominated and laminar, and the Nusselt equation (13) is used:

$$h_c = 1.47 \left[\frac{K_\ell^3 \rho_\ell (\rho_\ell - \rho_g) g}{\mu_\ell^2} \right]^{1/3} Re_c^{-1/3} \qquad (5\text{-}1)$$

At higher condensate rates the film becomes turbulent and the Colburn correlation (6) is the correct one to use. A curve fitted form of the Colburn correlation is:

$$h_c = 0.011 \left[\frac{K_\ell^3 \rho_\ell (\rho_\ell - \rho_g) g}{\mu_\ell^2} \right]^{1/3} Re_c^{1/3} \sqrt[4]{Pr_\ell} \qquad (5\text{-}2)$$

where:

$$Re_c = \frac{DG(1-x)}{\mu} \quad \text{and} \quad Pr_\ell = \left(\frac{C_p \mu}{K} \right)_\ell \qquad (5\text{-}3)$$

At high tube loadings the condensate film is vapor-shear controlled and the Boyko-Kruzhilin correlation (5) is valid:

$$h_c = 0.024 \left(\frac{DG}{\mu_\ell} \right)^{0.8} (Pr_\ell)^{0.43} \left[\frac{\sqrt{(\rho/\rho_m)_i} + \sqrt{(\rho/\rho_m)_o}}{2} \right] \qquad (5\text{-}4)$$

where:

$$\left(\frac{\rho}{\rho_m} \right)_i = 1 + \left(\frac{\rho_\ell - \rho_g}{\rho_g} \right) x_i \qquad (5\text{-}5)$$

and

$$\left(\frac{\rho}{\rho_m} \right)_o = 1 + \left(\frac{\rho_\ell - \rho_g}{\rho_g} \right) x_o \quad . \qquad (5\text{-}6)$$

The procedure is to calculate h_c by all the three equations and choose the higher value, since that is the one that is valid under existing conditions.

Inside Horizontal Tubes

For condensation inside horizontal tubes a procedure similar to

that suggested for vertical tubes is used. At low tube loadings (gravity dominated) the Kern correlation (11) is valid:

$$h_c = 0.761 \left[\frac{K_\ell^3 \rho_\ell (\rho_\ell - \rho_g) g L}{\mu_\ell W_T} \right]^{1/3} \qquad (5\text{-}7)$$

At high condensing loads, with vapor shear dominating, the Boyko-Kruzhilin correlation is valid. The procedure again is to calculate h_c from both equations and choose the higher value.

Outside Single Horizontal Tubes

Condensation on the outside of a single horizontal tube is satisfactorily handled by Nusselt's equation (13)

$$h_c = 1.51 \left[\frac{K_\ell^3 \rho_\ell (\rho_\ell - \rho_g) g}{\mu_\ell^2} \right]^{1/3} Re_c^{-1/3} \qquad (5\text{-}8)$$

where:

$$Re_c = \frac{4W}{\mu_\ell L} \quad . \qquad (5\text{-}9)$$

On Bank of Horizontal Tubes

The mean condensing coefficient for the entire row of N tubes is given by

$$h_{c,N} = h_{c,1} N^{-1/4} \quad .$$

This is much too conservative for values of N typical of process condensers. In roughly cylindrical bundles of horizontal tubes, the

usual practice is to use a mean value of the number of tubes in a vertical row, equal to 2/3 of the number of tubes in the central or longest row. There is a limited amount of proprietary data on the effect of vapor shear on horizontal tube banks. These indicate that at high velocities the condensing coefficient can be 10 to 20 times that predicted for the case of zero vapor shear.

For a preliminary rough design of a condenser, some typical values of film coefficients can be used. Table II gives film heat transfer coefficients for some of the substances commonly encountered in practice. Table III gives the typical overall heat transfer coefficients for tubular condensers (14). It is futile worrying too much about the precise value of a coefficient for preliminary design purposes. A better procedure for estimating U is to build up U from the individual h values, and wall, fin and fouling resistances using

$$\frac{1}{U_o} = \left(\frac{1}{h_o}\right) + R_{fo} + R_{fin} + \left(\frac{\Delta x}{K}\right)\left(\frac{A_o}{A_m}\right) + \left(R_{fi} + \frac{1}{h_i}\right)\left(A_o/A_i\right).$$

It will be generally found that one or at most two terms will dominate the value of U_o. Attention can be focussed upon these controlling values. For a very rough estimate of U_o the values given in Table IV can be used (3).

TABLE II

TYPICAL FILM HEAT TRANSFER COEFFICIENTS
FOR CONDENSATION

Component	h_c Btu/hr-ft^2-^{o}F
Propane	330
Propanol	350
Acetone	440
Benzene	320
Ammonia	1600
Water	2000
Carbon disulfide	380
Ethanol	500
Aniline	600-700
Dowtherm	250-300
Naphtha	200
Methanol	560

TABLE III

TYPICAL OVERALL HEAT TRANSFER COEFFICIENTS FOR TUBULAR CONDENSERS

Streams Involved		Design U_o
Shell Side	Tube Side	Btu/hr-ft^2-^{o}F
Alcohol Vapor	Water	100-200
Dowtherm Vapor	Tall Oil	60-80
Dowtherm Vapor	Dowtherm Liquid	80-120
Kerosene	Water	30-65
Naphtha	Water	50-75
Naphtha	Oil	20-30
Organic Solvents	Water	100-200
High Hydrocarbons	Water	20-50
Low Hydrocarbons	Water	80-200
Organic Solvents	Water	100-200
Steam	Water	400-1000
Sulfur Dioxide	Water	150-200
Steam	No. 2 Fuel Oil	60-90
Propane	Water	90-100
Air*	Freon-12	70
Air*	Ammonia	110
Air*	Gasoline	80
Air*	Light Hydrocarbons	90
Air*	Naphtha	75
Air*	Low Pressure Steam	135
Air*	Overhead Vapor	65

TABLE III (Continued)

Steams Involved		Design U_o
Shell Side	Tube Side	Btu/hr-ft^2-^{o}F
Gasoline	Water	80
Gas Oil	Water	50

*Finned tube coefficients based on inside area.

TABLE IV

OVERALL HEAT TRANSFER COEFFICIENTS FOR CONDENSATION

Streams		U_o
Fluid 1	Fluid 2	Btu/hr-ft^2-^{o}F
Water	Condensing Light Organic Vapors, Pure Component*	150-200
Water	Condensing Medium Organic Vapors, Pure Component*	100-150
Water	Condensing Heavy Organic Vapors, Pure Component*	75-100

*"Light Organic Liquids" include liquids with viscosities lesser than 0.5 cp.
"Medium Organic Liquids" include liquids with viscosities between 0.5 cp and 1.5 cp.
"Heavy Organic Liquids" include liquids with viscosities between 1.5 cp and 50 cp.
"Very Heavy Organic Liquids" include liquids with viscosities greater than 50 cp.

CHAPTER VI

RAPID ESTIMATION OF CONDENSER AREA

The basic design equation to be used for design is

$$A_o = \frac{Q}{U_o(MTD)} \tag{6-1}$$

The validity of this equation depends upon a number of assumptions, including constant specific heat of each stream and constant overall heat-transfer coefficient. These conditions are often not met. In principle, a more elaborate formulation is required. However, that completely defeats the purpose of rapid procedures, and most of these departures from ideality introduce errors smaller than the probable error in other approximations made.

Estimating A_o and Key Exchanger Parameters

Once Q, MTD and U_o are known the total outside heat transfer area A_o is readily found from Equation 6-1. Figure 22 can be used to select the heat exchanger dimensions corresponding to the calculated A_o (3). In this figure the ordinate is A_o, in ft^2, and the abscissa is the effective tube length (tube sheet to tube sheet for straight tube bundles, or length of a single straight section from tube sheet to tangent line for a U-tube bundle) in ft.

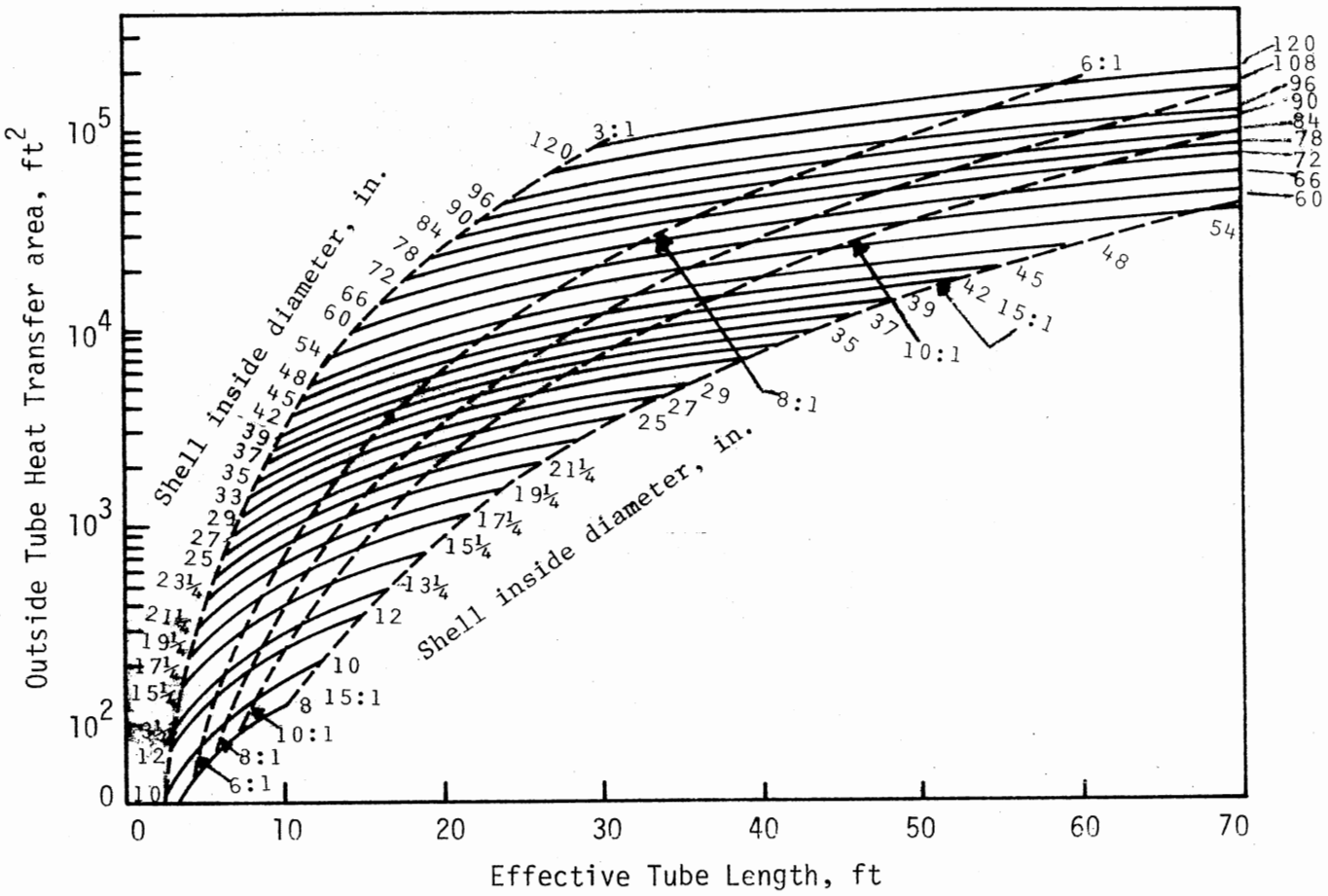

Figure 22. Heat Transfer Area Versus Effective Tube Length

The solid black lines in parameters are the commonly specified shell inside diameters in inches. Using standard tube count tables for 3/4-in OD tubes on a 15/16-in triangular pitch for a fixed-tube-sheet heat exchanger with one tube pass, the total outside tube area that can be fitted into a shell has been calculated.

Therefore, once the required area A_o is known, Figure 11 shows immediately the combinations of tube length and the shell diameter that will provide the area in a single shell for an exchanger of the given tube size and layout. The dashed lines in parameter in Figure 22 show the approximate locus of shells having a given effective tube length to shell diameter ratio. Many heat exchangers fall into the 6:1 to 8:1 range, with a pronounced trend towards the higher values as pressure drop prediction procedures have improved.

Extension of Figure 22

Figure 22 can be used to estimate the required length and diameter of exchangers for other tube sizes and layouts, multiple tube side passes and different bundle constructions. An effective area, A_o', is defined by

$$A_o' = A_o F_1 F_2 F_3 \qquad (6\text{-}2)$$

where:

A_o' = the area on the ordinate of Figure 22

A_o = the required outside area as calculated from Equation 6-1

F_1 = the correction factor for the unit cell tube array

F_2 = the correction factor for the number of tube passes

F_3 = the correction factor for the shell construction/tube bundle layout type.

Values of the correction factors are given in Table V (F_1), Table VI (F_2), and Table VII (F_3). It should be emphasized that the use of this technique is approximate, especially for the smaller-diameter shells.

Therefore, for preliminary estimates one could get the heat exchanger dimensions for a given area using this technique. This rapid preliminary estimate will be adequate for many purposes.

TABLE V

F_1 FOR VARIOUS TUBE LAYOUTS AND DIAMETERS

Tube OD, in.	Tube Pitch, in.	Layout	F_1
5/8	13/16	→ ◁	0.90
5/8	13/16	→ □ ◇	1.04
3/4	15/16	→ ◁	1.00
3/4	15/16	→ □ ◇	1.16
3/4	1	→ ◁	1.14
3/4	1	→ □ ◇	1.31
1	1 1/4	→ ◁	1.34
1	1 1/4	→ □ ◇	1.54

TABLE VI

F_2 FOR VARIOUS NUMBERS OF TUBE-SIDE PASSES

Inside Shell Diameter, in.	Number of Tube-Side Passes			
	2	4	6	8
Up to 12	1.20	1.40	1.80	--
13 1/4 to 17 1/4	1.06	1.18	1.25	1.50
19 1/4 to 23 1/4	1.04	1.14	1.19	1.35
25 to 33	1.03	1.12	1.16	1.20
35 to 45	1.02	1.08	1.12	1.16
48 to 60	1.02	1.05	1.08	1.12
Above 60	1.01	1.03	1.04	1.06

TABLE VII

F_3 FOR VARIOUS TUBE-BUNDLE CONSTRUCTIONS

Type of Tube Bundle Construction	Inside Shell Diameter, in.				
	Up to 12	13 1/4-21 1/4	23 1/4-35	37-48	Above 48
Split Backing Ring (TEMA S)	1.30	1.15	1.09	1.06	1.04
Outside Packed Floating Head (TEMA P)	1.30	1.15	1.09	1.06	1.04
U-Tube (TEMA U)	1.12	1.08	1.03	1.01	1.01
Pull-Through Floating Head (TEMA T)	--	1.40	1.25	1.18	1.15

CHAPTER VII

OPTIMIZATION PROCEDURES

Since condensers are major pieces of equipment, the design of condensers based on the minimum total cost is most appropriate. Process economic feasibility studies usually evaluate several alternatives in which heat exchanger calculations occur frequently. The use of the principles of price optimum design and the computer greatly reduce the time required for these calculations and eliminate mistakes.

Price Optimum Design

Price optimum design (15) is that design having the lowest cost in terms of annual fixed and variable costs. By fixing the design requirements at various alternate values and comparing the costs, an economic design can be found.

For example, the initial conditions usually given are:

1. Vapor flow rate
2. Total amount of vapor to be condensed
3. Inlet temperature of the utility fluid.

The parameters required are:

1. Heat transfer area
2. Exit temperature of the utility fluid
3. Flow rate of the utility fluid

4. Number, length of tubes, tube size and tube layout
5. Shell diameter
6. Shell side and tube side pressure drops.

The most direct approach is to determine the design on a price optimum basis initially.

Optimum economic design implies the best or most favorable conditions, and usually optimum conditions can be reduced to a consideration of costs.

Outline of Optimization Procedure

The total heat exchanger cost to be minimized includes the annual fixed charges and annual variable operating costs. Annual fixed charges are those costs which remain constant, including depreciation, taxes, insurance and rent. Plant overheat costs are similar and may be included in this category. Annual variable operating costs are those items directly dependent on the production rate, including the cost of the utility fluid, the costs for pumping, direct labor and maintenance. The detailed procedure for optimization of condensers is given in Reference (15). It is suggested that the designer use better design correlations than given in this Reference. The following information may be specified before one starts to optimize a condenser:

1. Tube diameter, wall thickness, pitch and tube layout
2. Number of tube passes
3. Heat-transfer resistance caused by tube walls, dirt and scale.

The calculation procedure gives the following optimum values:

1. Optimum h_i
2. Optimum h_o
3. Optimum U_o
4. Optimum mass velocities for tube side and shell side
5. Optimum flow rate of utility fluid
6. Optimum number of tubes and minimum cross flow area on the shell side
7. Optimum length of tubes.

Optimum tube size is not determined since the tube size does not affect the total cost very much.

Important Features of Condenser Optimization

In the case of condensers, there are some simplifications possible which reduce the number of independent variables in the total cost equation (15). The power cost for the condensing fluid side can be considered to be negligible. Also, for a preliminary and rough optimization, the temperature of the condensing side can be considered to be constant. Another reasonable assumption possible is that since the heat transfer resistance of the condensing fluid film is relatively small in most cases, a reasonable constant value for the condensing film coefficient can be assumed. Thus, in the case of condensers, the number of independent variables in the design is reduced to two.

This procedure is an approximate procedure and a very rigorous procedure should include the effect of pressure drop on condensing film coefficient and mean temperature difference. This effect has been

discussed in Chapter II and Chapter III of this thesis. The incorporation of equations for the effect of pressure drop on h_c and MTD into the optimization program discussed earlier will give rise to a better optimized design of a condenser.

Limitations of Price Optimum Design

Since price optimum design is based on costs, the reliability of the design depends on the accuracy of the fixed charges, the accuracy of the variable operating costs, and the accuracy of the installed cost of the condenser. The source of data on these costs has a significant effect on the final result of the optimization of condensers.

CHAPTER VIII

SUMMARY AND CONCLUSIONS

This thesis deals with approximate design estimates for pure component condensers.

The various aspects involved in condensation of pure component vapors are studied. The effect of pressure drop on the heat transfer coefficient and on the mean temperature difference is studied. It is found that increase in pressure drop increases heat transfer coefficient and decreases mean temperature difference. The increase or decrease depends upon various factors discussed in this thesis. A rapid estimation procedure for design of condensers and calculation of pressure drop is presented. Finally, a discussion on optimization of condensers is presented.

The methods outlined in this thesis give a quick estimate useful as a first step in obtaining a more exact design. These rapid estimates are particularly useful when a designer is doing a very preliminary estimate of plant cost, layout and space requirements.

SELECTED BIBLIOGRAPHY

1. Alves, G. E., "Cocurrent Liquid-Gas Flow in a Pipe-Line Contactor," Chem. Eng. Prog. 50, No. 9, 449 (1954).

2. Baker, O., "Simultaneous Flow of Oil and Gas," The Oil and Gas J. 53, No. 12, 185 (1954).

3. Bell, K. J., "Estimate S&T Exchanger Design Fast," The Oil and Gas Journal, 59 (December, 1978).

4. Bell, K. J., "Final Report of the Cooperative Research Program on Shell and Tube Heat Exchangers, University of Delaware," University of Delaware Eng. Exp. Station, Bulletin, No. 5 (June, 1963).

5. Boyko, L. D. and Kruzhilin, G. N., "Heat Transfer and Hydraulic Resistance During Condensation of Steam in a Horizontal Tube and Bundle of Tubes," Int. Journal of Heat and Mass Transfer 10, 361 (1967).

6. Colburn, A. P., "Note on the Calculation of Condensation When a Portion of the Condensate Layer is in Turbulent Motion," Trans. AIChE 30, 187 (1934).

7. Colburn, A. P. and Hougen, O. A., "Design of Cooler Condensers for Mixtures of Vapors of Noncondensing Gases," Ind. Eng. Chem. 26, 1178 (1934).

8. Diehl, J. E., "Calculate Condenser Pressure Drop," Petroleum Refiner 36, No. 10, 147 (1957).

9. Diehl, J. E. and Unruh, C. H., "Two-Phase Pressure Drop for Horizontal Crossflow Through Tube Banks," Petroleum Refiner 37, No. 10, 124 (1958).

10. Fair, J. R., "What You Need to Design Thermosiphon Reboilers," Pet. Ref. 39, No.-2, 105 (1960).

11. Kern, D. Q., Process Heat Transfer, New York: McGraw Hill Book Company, 256-266 (1950).

12. Martinelli, R. C. and Nelson, D. B., "Prediction of Pressure Drop During Forced-Circulation Boiling of Water," Trans. ASME 70, 695 (1948).

13. Nusselt, W., "The Surface Condensation of Steam," Zeits. V.D.I. 60, No. 27, 541 (1916).

14. Perry, R. H. and Chilton, C. H., Eds., Chemical Engineer's Handbook, 5th Ed., New York: McGraw-Hill Book Co. (1973).

15. Peters, M. S. and Timmerhaus, K. D., Plant Design and Economics for Chemical Engineers, 2nd Ed., New York: McGraw-Hill Book Co., 574-595 (1968).

16. Private communication with K. J. Bell, Oklahoma State University, Stillwater, Oklahoma, 1979.

APPENDIX A

TUBE SIDE PRESSURE DROP CALCULATIONS

Based on Liquid Phase

$$\left(\frac{dp}{d\ell}\right)_{f,\ell} = \frac{2f_\ell G_\ell^2}{g_c D\rho_\ell} \Phi^2_{\ell tt} \tag{A-1}$$

$\Phi^2_{\ell tt}$ is read from Figure 9 for the value of $\sqrt{\chi_{tt}}$ calculated by

$$\sqrt{\chi_{tt}} = \left(\frac{1-x}{x}\right)\left(\frac{\rho_v}{\rho_\ell}\right)^{0.57}\left(\frac{\mu_\ell}{\mu_v}\right)^{0.11} \tag{A-2}$$

$$\chi_{tt} = \left(\frac{1-x}{x}\right) R_1 \tag{A-3}$$

$$\therefore \Delta P_{TPF} = \frac{2G^2 f}{g_c D\rho_\ell} \int_o^L (1-x)^2 \Phi^2_{\ell tt}\, d\ell \tag{A-4}$$

$$\therefore \Delta P_{TPF} = \frac{2fG^2}{g_c D\rho_\ell} \int_o^L (1-x)^2 \Phi^2_{\ell_{tt}} \left(\frac{d\ell}{dx}\right) dx \tag{A-5}$$

Assuming linear condensation rate

$$\frac{dx}{d\ell} = \frac{1}{L} \tag{A-6}$$

$$\Delta P_{TPF} = \frac{2fG^2 L}{g_c D\rho_\ell} \int_1^x (1-x)^2 \Phi^2_{\ell tt}\, dx \tag{A-7}$$

$$\Delta P_{TPF} = \frac{2fG^2 L}{g_c D\rho_\ell} \overline{\Phi^2_{\ell tt}} \tag{A-8}$$

where

$$\overline{\Phi^2_{\ell tt}} = \int_1^x (1-x)^2 \Phi^2_{\ell tt}\, dx \tag{A-9}$$

This integral is evaluated at different values of R_1 and for different

exit vapor qualities. The results are shown on Figure 10.

Based on Vapor Phase

$$\left(\frac{dp}{d\ell}\right)_{f,v} = \frac{2fG_v^2}{g_c D\rho_v} \Phi_{\ell tt}^2 \chi_{tt}^{1.75} \tag{A-10}$$

$$\left(\frac{dp}{d\ell}\right)_{f,v} = \frac{2fG^2x^2}{g_c D\rho_v} \Phi_{\ell tt}^2 \chi_{tt}^{1.75} \tag{A-11}$$

Proceeding in a similar fashion as for the liquid phase we have

$$\Delta P_{TPF} = \frac{2fG^2L}{g_c D\rho_v} \Phi_{\ell tt}^2 \tag{A-12}$$

where

$$\overline{\Phi_{\ell tt}^2} = \int_1^x x^2 \chi_{tt}^{1.75} \Phi_{\ell tt}^2 \, dx \tag{A-13}$$

This integral is evaluated at different values of R_1 and for different exit vapor qualities. The results are shown on Figure 11.

Based on Liquid Phase Considering
Variation of Friction Factor

Assuming liquid phase is in the turbulent region, one can substitute in equation A-4.

$$f = \frac{0.078}{(DG_\ell/\mu_\ell)^{0.25}} \tag{A-14}$$

Equation A-4 simplifies to

$$\Delta P_{TPF} = \frac{0.156\mu_{\ell}^{0.25} L G^{1.75}}{D^{1.25} g_c \rho_{\ell}} \int_1^x (1-x)^{1.75} \Phi_{\ell tt}^2 \, dx \qquad \text{(A-15)}$$

$$\therefore \Delta P_{TPF} = \frac{0.156\mu_{\ell}^{0.25} L G^{1.75}}{D^{1.25} g_c \rho_{\ell}} \overline{\Phi_{\ell tt}^2} \qquad \text{(A-16)}$$

where

$$\overline{\Phi_{\ell tt}^2} = \int_1^x (1-x)^{1.75} \Phi_{\ell tt}^2 \, dx \qquad \text{(A-17)}$$

This integral is evaluated for different values of R_1 at different values of exit vapor qualities and the results are shown in Figure 12.

Based on Vapor Phase Considering Variation of Friction Factor

Assuming vapor phase is in the turbulent region, one can substitute in equation A-11,

$$f = \frac{0.078}{(DG_v/\mu_v)^{0.25}} \qquad \text{(A-18)}$$

and proceeding in the same fashion as for the liquid phase we have

$$\Delta P_{TPF} = \frac{0.156\mu_{v}^{0.25} L G^{1.75}}{D^{1.25} g_c \rho_{v}} \overline{\Phi_{\ell tt}^2} \qquad \text{(A-19)}$$

where

$$\overline{\Phi^2_{\ell tt}} = \int_1^x x^{1.75}\, X_{tt}^{1.75}\, \Phi^2_{\ell tt}\, dx \qquad \text{(A-20)}$$

This integral is evaluated for different values of R_1 at different values of exit vapor qualities and the results are shown in Figure 13.

APPENDIX B

SHELL SIDE PRESSURE DROP CALCULATIONS

In the paper by Diehl and Unruh (13) two phase pressure drop across tube banks has been studied and a graph of $\frac{\Delta P_{TPF}}{\Delta P_g}$ against $LVF/(\rho_g/\rho_\ell)$ is plotted for different tube layouts (Figure 14). The liquid volume fraction LVF is defined by

$$LVF = \frac{\omega_\ell/\rho_\ell}{\frac{\omega_\ell}{\rho_\ell} + \frac{\omega_v}{\rho_v}} \tag{B-1}$$

$$\therefore LVF = \frac{G(1-x)/\rho_\ell}{\frac{G(1-x)}{\rho_\ell} + \frac{Gx}{\rho_v}} \tag{B-2}$$

$$\therefore LVF = \frac{1}{1 + \frac{\rho_\ell}{\rho_v}\,\frac{x}{1-x}} \tag{B-3}$$

Define R_2 as

$$R_2 = \frac{\rho_\ell}{\rho_v} \tag{B-4}$$

$$LVF = \frac{1}{1 + \frac{R_2 x}{1-x}} \tag{B-5}$$

Abscissa of Figure 14 is $\dfrac{R_2}{1 + \frac{R_2 x}{1-x}}$

Define $\Phi^2_{\ell tt} = \dfrac{\Delta P_{TPF}}{\Delta P_g}$ (B-6)

$$d(\Delta P_{TPF}) = d(\Delta P_g)\ \Phi^2_{\ell tt} \tag{B-7}$$

$$\Delta P_{TPF} = \Delta P_g \int_1^x \Phi^2_{\ell tt}\ x^2\ dx \tag{B-8}$$

$$\Delta P_{TPF} = \Delta P_g\ \overline{\Phi^2_{\ell tt}} \tag{B-9}$$

where

$$\overline{\Phi^2_{\ell tt}} = \int_1^x x^2\ \Phi^2_{\ell tt}\ dx \tag{B-10}$$

and

ΔP_g is the pressure drop assuming only vapor flows with total mass velocity G.

The integral is evaluated for different values of $R_2 (= \frac{\rho_\ell}{\rho_v})$ and different values of exit vapor quality. It was found that results did not vary much with R_2 and therefore results corresponding to R_2 equal to 30 are considered sufficient and are shown in Figure 15. The results were studied for variation of R_2 from 10 to 1000. Also, the results did not vary much with tube orientation and therefore average values of $\Delta P_{TP}/\Delta P_g$ were taken for calculations from Figure 14.

APPENDIX C

SAMPLE CALCULATIONS

Example Problem 1.

It is desired to totally condense 50,000 lb/hr of saturated propane vapor at $105^{o}F$ and 200 psia on the shell side of a shell and tube heat exchanger, by heating cooling water from $80^{o}F$ to $100^{o}F$. A fixed tube sheet heat exchanger is specified. The tube size and layout is specified as 3/4-in. OD 16BWG tubes on a 1-in. equilateral triangular pitch.

Estimate the shell length, shell diameter and the shell side pressure drop. The properties of saturated propane at these conditions are as follows:

$$\Delta H_v = 138 \text{ Btu/lb}$$
$$\rho_v = 1.85 \text{ lb/ft}^3$$
$$\rho_\ell = 29.3 \text{ lb/ft}^3$$
$$K_\ell = 0.074 \text{ Btu/hr ft}^{o}F$$
$$\mu_\ell = 0.08 \text{ centipoise}$$
$$\mu_v = 0.0085 \text{ centipoise}$$

Solution:

$$\text{Condenser duty } Q = 50{,}000\ (138)$$
$$= 6.9 \times 10^6 \text{ Btu/hr}$$

$$\text{The flow rate of cooling water} = 6.9 \times 10^6/(100-80)(1)$$
$$= 3.45 \times 10^5 \text{ lb/hr}$$

Mean temperature difference:

$$LMTD = [(105-80)-(105-100)]/\ell n[(105-80)/(105-100)]$$

$$= 12.43^{o}F$$

U_o from Table IV is 200 Btu/hr ft^2 ^{o}F

Calculation of the required area:

$$A_o = (6.9 \times 10^6)/(200)(12.43)$$

$$= 2780\ ft^2$$

This is the area required in the actual exchanger. But, in order to use Figure 22 it is necessary to use Equation 6.3 and the associated tables to find A_o'.

From Table V for 3/4-in. OD tubes on 1-in. equilateral triangular pitch, $F_1 = 1.14$. From Table VI for four tube passes and 25 to 33-in. shell, $F_2 = 1.12$. Since fixed tube sheet construction is specified, $F_3 = 1.0$.

Therefore:

$$A_o' = 2,780(1.14)(1.12)(1.0)$$

$$= 3,550\ ft^2.$$

Entering Figure 22 at 3,550 ft^2 on the ordinate, the following shell diameter/length combinations will provide the required area:

Shell ID, in.	Tube Length, ft.	L/D_i
39	12	3.7
37	14	4.5
35	16	5.5
33	17	6.2
31	20	7.7
29	24	10.0
27	27	12.0
25	31	14.9

The 31-in. ID shell, 20 ft. long would probably represent typical practice in the case, but those on either side would likely prove equally feasible.

It is worth checking the velocity of water in the tubes. Using a standard tube count table from Reference 16, there are 678 tubes for four tube passes. The velocity of water in the tubes would be:

$$(3.45 \times 10^5)/(678/4)(\pi/4)(0.62/12)^2(3600)(62)$$
$$= 4.35 \text{ ft/sec.}$$

which is in line for water. One could go further and calculate the shell side pressure drop.

Using a standard table from Reference 16,

$$p_p = 0.866$$
$$p_N = 0.5$$

Using a 12-in. baffle spacing, Equation 4.18 gives

$$S_m = (31)(0.25)(12)/(0.5)$$
$$= 186 \text{ in}^2.$$

Equation 4.19 gives

$$S_w = 186 \text{ in}^2.$$
$$Re_s = 12\ (0.75)(50,000)/(0.0085)(2.42)(186)$$
$$= 58,800$$

Equation 4.22 gives

$$f_i = 0.1$$

$$N_b = 12(20)/(12)-1$$

$$= 19$$

Using a 30 percent baffle cut

$$N_c = 31\ [1-2(0.3)]/(0.866)$$

$$= 14$$

$$N_{cw} = 0.8(0.3)(31)/(0.866)$$

$$= 9$$

Therefore:

$$\Delta P_g = 0.69 \times 10^{-6}(0.1)(50{,}000)^2(14)/(1.85)(186)^2$$

$$= 3.77 \times 10^{-2}\ \text{lbf/in.}^2$$

$$\Delta P_{g,w} = 1.73 \times 10^{-7}(50{,}000)^2[2+0.6(9)]/(186)(186)(1.85)$$

$$= 5 \times 10^{-2}\ \text{lbf/in.}^2$$

Equation 4.20 and 4.21 give

$$R_{ST,CF} = 0.45$$

$$R_{ST,W} = 0.6$$

R_1 from Equation 4.10 is

$$(1.85/29.316)^{0.57}(0.08/0.0085)^{0.11}$$

$$= 0.265$$

From Figure 11 for x=0 and $R_1 = 0.265$

$$\overline{\Phi^2_{\ell tt}} = 1.2$$

From Figure 15 for x=0

$$\overline{\Phi^2}_{\ell tt,CF} = 0.29.$$

Therefore:

$$\Delta P_{TPF} = [(0.0377)(0.45)(0.29)](20) + [(0.05)(1.2)(0.6)](19)$$
$$= 0.78 \text{ lbf/in.}^2$$

Therefore, for preliminary estimates one could specify that a fixed tube sheet exchanger, 31-in. inside shell diameter by 20 ft. long (tube sheet to tube sheet) containing 678 tubes 3/4-in. OD 16 BWG on a 1-in. equilateral triangular pitch, four tube side passes would be adequate. This construction gives a shell side pressure drop of 0.78 lbf/in.^{2}. This much information will be sufficient for many purposes.

Example Problem 2

It is required to condense 300 lb/hr of saturated propane vapor at 105^{o}F and 200 psia inside a 3/4-in. OD 16 BWG tube 50 ft. long. Estimate the frictional pressure drop. The properties of propane are same as in problem 1.

The flow area of the tube = 0.302 in.^{2}.

Total mass velocity G = 300/(0.302/144)

$$= 1.43 \times 10^5 \text{ lb/hr-ft}^2$$

$$Re_{\ell} = (0.62/12)(1.43 \times 10^5)/(0.08)(2.42)$$
$$= 3.82 \times 10^4 \text{ which is greater than 2100.}$$

Therefore, the calculations are based on the liquid phase.

From Figure 9 for this Reynolds number

$$f = 0.0055$$

$\overline{\Phi^2_{\ell tt}}$ for x=0 and $R_1 = 0.265$ is 12.0 from Figure 10.

Therefore, Equation 4.9 gives

$$\Delta P_{TPF} = 12 \left[\frac{(4)(0.0055)(1.43 \times 10^5)^2 (50)}{(2)(4.17 \times 10^8)(0.62/12)(29.3)} \right]$$

$$= 213.8 \text{ lbf/ft}^2$$

$$= 1.5 \text{ lbf/in.}^2 \quad .$$

This gives a quick and approximate estimate of the pressure drop.

VITA[2]

Suresh Balakrishnan

Candidate for the Degree of

Master of Science

Thesis: APPROXIMATE DESIGN ESTIMATES FOR PURE COMPONENT CONDENSERS

Major Field: Chemical Engineering

Biographical:

Personal Data: Born in Bombay, India, February 10, 1955, the son of Mr. and Mrs. Balakrishman Nair.

Education: Graduated from South Indian Welfare Society's High School, Bombay, India, in May, 1971; received Bachelor of Technology degree in Chemical Engineering from Indian Institute of Technology, Bombay, India, in June, 1977; completed requirements for the Master of Science degree at Oklahoma State University in July, 1979.

Professional Experience: Trainee Engineer for Mercury Paints, Bombay, India in the summer of 1975 and for National Organic Chemicals United, Bombay, India, in the summer of 1976; Senior Project Assistant with Indian Institute of Technology, Bombay, India, in the summer of 1977; Process Engineer with Union Carbide, Bombay, India, from December, 1977 to August 1978; Graduate Assistant, Oklahoma State University, School of Chemical Engineering, from September, 1978, to July, 1979.